

MATHEMATISCHES FORSCHUNGSINSTITUT OBERWOLFACH

Report No. 39/2020

DOI: 10.4171/OWR/2020/39

**Computational Inverse Problems for
Partial Differential Equations
(hybrid meeting)**

Organized by
Liliana Borcea, Ann Arbor
Thorsten Hohage, Göttingen
Barbara Kaltenbacher, Klagenfurt

6 December – 12 December 2020

ABSTRACT. Inverse problems in partial differential equations (PDEs) consist in reconstructing some part of a PDE such as a coefficient, a boundary condition, an initial condition, the shape of a domain, or a singularity from partial knowledge of solutions to the PDE. This has numerous applications in nondestructive testing, medical imaging, seismology, and optical imaging. Whereas classically mostly boundary or far field data of solutions to deterministic PDEs were considered, more recently also statistical properties of solutions to random PDEs have been studied. The study of numerical reconstruction methods of inverse problems in PDEs is at the interface of numerical analysis, PDE theory, functional analysis, statistics, optimization, and differential geometry. This workshop has mainly addressed five related topics of current interest: model reduction, control-based techniques in inverse problems, imaging with correlation data of waves, fractional diffusion, and model-based approaches using machine learning.

Mathematics Subject Classification (2010): 35xx, 45xx, 47xx, 49xx, 65xx, 78xx, 80xx, 86xx.

Introduction by the Organizers

The workshop *Computational Inverse Problems for Partial Differential Equations*, organised by Liliana Borcea (Ann Arbor), Thorsten Hohage (Göttingen) and Barbara Kaltenbacher (Klagenfurt) was well attended with over 44 participants. The pandemic situation at the time of the workshop allowed only people from Germany to participate without at least 5 days of quarantine. Therefore, the meeting was carried out in a hybrid format. Seven participants came to Oberwolfach, among

them one woman and two from outside of Germany. In addition, 37 participants, among them 9 women, attended the workshop online. To allow numerous participants from Northern and Central America to follow talks at reasonable times, the sessions were scheduled in the afternoons and evenings European time, despite of the inconvenience for two participants from Asia.

Online attendance during the talks was quite good. Furthermore, we had lively debates in three discussion sessions. However, virtual break-out rooms to allow coffee-break talks for online participants were hardly used.

Let us first summarize the talks and discussions in the five focus areas:

- Inverse problems with fractional diffusion:
PDEs containing fractional derivatives have recently found much interest due to their relevance in a wide range of applications. Fractional diffusion arises, e.g., phenomenological in the context of power law frequency dependent attenuation, but also first principles based, as a macroscopic limit of continuous time random walks with non-Gaussian increments. Mathematically, this results in non-local operators, whose numerical and analytic treatment requires tools that are to some extent parallel to their local counterparts, e.g., in variational and energy based PDE theory and numerics. To a large extent they are yet to be developed, though, for example when it comes to defining boundary conditions that often play the role of observations in inverse problems, or in the presence of nonlinearities. Besides the immediate impact of such PDE techniques onto inverse problems for PDEs, there are also inherent inverse problems questions like ill-posedness and uniqueness, that turn out to sometimes yield very different answers as soon as fractional derivative terms arise in the models. Also the stochastically and physically (biologically, economically etc.) correct modeling of anomalous diffusion itself is a crucial step in which inverse methods can and should be involved. These and further questions have been addressed in a discussion session chaired by William Rundell.
- Optimal control techniques:
A vast majority of regularization methods are based on the minimization of a combination of functionals penalizing deviation from the observed data, counteracting the ill-posedness, and enhancing desired features of quantities to be reconstructed. Thus, the synergies between inverse problems and optimal control are obvious on the level of computational methodology. More specifically, in view of the fact that forward models often consist of (partial) differential equations, there are strong common interests with PDE constrained optimization also on the analytical side. Recent findings on regularization with - sometimes statistics based - nonsmooth and nonconvex cost functions as well as constraints have inspired advances in optimization methodology. On the other hand, methodology from optimization theory such as duality based reasoning or the use of properties of Lagrange multipliers are about to find their way into regularization theory. Joint interests and distinguishing features were highlighted in a discussion

session on “Optimal control, optimization, and inverse problems” chaired by Christian Clason.

- Reduced order modeling:

Reduced order modeling is a methodology that has been driven by the computational dynamical systems and linear algebra community. Recently it has emerged as a promising tool for solving inverse problems. There are two ideas that have been pursued, and both were represented in the workshop: The first idea is to obtain an algebraic model, a matrix of small size, for the forward mapping from the coefficients in the PDE to the measurements. This facilitates fast forward model evaluations which are important for example in optimization approaches to solving inverse problems. The second idea seeks a matrix as a reduced order model of the PDE operator. This can be done in a data driven way (i.e., using only the measurements given in the inverse problem) and moreover, the reduced order model can be built so that it inherits important properties of the PDE operator which can then be exploited for inversion.

- Correlation based imaging:

Correlation based imaging has emerged over the past 20 years as a powerful technique for solving inverse problems for wave equations with randomly fluctuating wave speed and impedance. Various imaging modalities have been proposed, and they all rely on the assumption that with careful statistical smoothing techniques such as windowing and convolutions, the empirical correlations of wave components (modes) are statistically stable, meaning that they are approximated by statistical second moments. This assumption generically holds in mixing random media (i.e., with rapidly decaying correlation function of the fluctuations). However, there are systems, such as open waveguides that arise in shallow water acoustics, where coupling between the propagating modes and the modes that radiate in the ocean floor breaks the assumption. One presentation in the workshop introduced and analyzed mathematically this important discovery. Another presentation in the workshop considered a situation where the assumption holds. In particular, it described the mathematics of beam propagation at long distance in random media and how it can be used for understanding emerging techniques like speckle imaging.

- Model-based approaches using machine learning:

Despite the tremendous success of machine learning, and in particular deep learning methods in many areas of imaging sciences, a straightforward application of such methods to inverse problems in PDEs is usually not competitive. The challenge is to incorporate our understanding of nature modelled by partial differential equations into machine learning approaches. This provides the opportunity to learn from large data sets under the constraint of the laws of nature, and may lead to significantly improved results. An example addressed in one of the talks are special neural network architectures for approximating highly nonlinear functions

whose inputs are linear operators. Such so-called operator recurrent neural networks can be used for the solution of nonlinear inverse problems in wave equations with operator-valued data. A discussion session on “Potential and limitations of data-driven approaches in inverse problems” organized by Peter Maaß focused on the integration of model based expert knowledge into data-driven concepts, a regularization theory for neural network based approaches, and mathematical concepts for addressing novel challenges in data-driven inverse problems.

In addition to these focus areas, topics such as the reconstruction of singularities either in electrical impedance tomography or in geophysics, lower bounds on the feasibility of broadband passive cloaking, magnetic particle imaging, and reaction-diffusion models for cancer prediction were addressed.

Workshop (hybrid meeting): Computational Inverse Problems for Partial Differential Equations

Table of Contents

| | |
|--|------|
| Harbir Antil | |
| <i>Role of Fractional Operators in Inverse Problems</i> | 1909 |
| Elena Beretta (joint with Andrea Aspri, Anna Mazzucato, Maarten de Hoop) | |
| <i>Analysis of a model of elastic dislocations in geophysics</i> | 1911 |
| George Biros (joint with Shashank Subramanian, Klaudius Scheufele, Miriam Mehl) | |
| <i>Where did the tumor start? Sparse reconstruction of initial conditions for reaction-diffusion PDEs</i> | 1912 |
| Maxence Cassier (joint with Graeme W. Milton) | |
| <i>Bounds on Herglotz functions and physical limits to broadband passive cloaking in the quasistatic regime</i> | 1913 |
| Herbert Egger (joint with Jürgen Dölz, Matthias Schlottbom) | |
| <i>On model reduction for tomographic inverse problems</i> | 1916 |
| Josselin Garnier | |
| <i>Wave Propagation and Correlation-based Imaging in Random Media: From Gaussian to non-Gaussian Statistics</i> | 1918 |
| Maarten V. de Hoop (joint with Matti Lassas, Christopher A. Wong) | |
| <i>Deep learning architectures for nonlinear operator functions and nonlinear inverse problems</i> | 1919 |
| Bangti Jin (joint with Zhi Zhou) | |
| <i>Numerical analysis of diffusion coefficient identification for elliptic and parabolic systems</i> | 1920 |
| Tobias Kluth (joint with Hannes Albers) | |
| <i>Simulation of non-linear magnetization effects and parameter identification problems in magnetic particle imaging</i> | 1922 |
| Roman Novikov (joint with Petr Grinevich, Iskander Taimanov) | |
| <i>Moutard transform for the generalized analytic functions and for the conductivity equation</i> | 1925 |
| Hans-Georg Raumer (joint with Thorsten Hohage, Carsten Spehr, Daniel Ernst) | |
| <i>Numerical Methods for Source Power Reconstruction in Experimental Aeroacoustics</i> | 1928 |

| | |
|---|------|
| Kui Ren (joint with Ru-Yu Lai, Yimin Zhong, Ting Zhou) | |
| <i>Inverse Problem for Semilinear Radiative Transport with Internal Data</i> | 1930 |
| William Rundell (joint with Barbara Kaltenbacher) | |
| <i>The influence of a fractional subdiffusion operator: A tale of two inverse problems</i> | 1933 |
| Otmar Scherzer (joint with Clemens Kirisits, Michael Quellmalz, Monika Ritsch-Marte, Eric Setterqvist, Gabriele Steidl) | |
| <i>Reconstruction formulae for diffraction tomography with optical tweezers</i> | 1934 |
| Marian Slodička (joint with Katarina Šišková) | |
| <i>Some inverse source problems in semilinear fractional PDEs</i> | 1936 |
| Knut Sølna (joint with Josselin Garnier) | |
| <i>Beam Propagation in Random Media with Applications to Imaging and Communication</i> | 1938 |
| Chrysoula Tsogka (joint with Miguel Moscoso, Alexei Novikov and George Papanicolaou) | |
| <i>The Noise Collector for sparse recovery in high dimensions</i> | 1941 |
| Daniel Wachsmuth (joint with Carolin Natemeyer) | |
| <i>Proximal gradient methods applied to optimization problems with L^p-cost, $p \in [0, 1)$</i> | 1942 |
| Anne Wald (joint with Tram T. N. Nguyen, Barbara Kaltenbacher, Thomas Schuster) | |
| <i>Parameter identification for the Landau-Lifshitz-Gilbert equation in Magnetic Particle Imaging</i> | 1944 |
| Jörn Zimmerling (joint with Liliana Borcea, Vladimir Druskin) | |
| <i>A reduced order model approach to inverse scattering in lossy layered media</i> | 1947 |

Abstracts

Role of Fractional Operators in Inverse Problems

HARBIR ANTIL

Nonlocal (fractional) operators such as fractional Laplacian and fractional time derivative have shown remarkable promise in many applications in capturing anomalous behavior and processes involving jump across the interfaces. In complex/heterogeneous material mediums, the long-range correlations or hereditary material properties are presumed to be the cause of this anomalous behavior. Besides being able to capture long range effects, these operators enforce less smoothness than their classical counterparts.

We begin this talk by introducing various definitions of fractional Laplacian in a bounded domain $\Omega \subset \mathbb{R}^N$ with boundary $\partial\Omega$. There are several ways to define fractional Laplacian in this setting, we consider the two most popular ones. With fractional exponent $s \in (0, 1)$, we first define the *Spectral fractional Laplacian* as

$$(-\Delta)^s u = \sum_{k=1}^{\infty} \lambda_k^s u_k \varphi_k$$

where $u_k = \int_{\Omega} u \varphi_k dx$, with $\{(\lambda_k, \varphi_k)\}_{k=1}^{\infty}$ denoting the eigenvalues and eigenfunctions of the standard Laplacian with zero Dirichlet conditions, i.e., $-\Delta \varphi_k = \lambda_k \varphi_k$ in Ω and $\varphi_k = 0$ on $\partial\Omega$. The second definition is the so-called *Integral fractional Laplacian* given by

$$(-\Delta)^s u(x) = C_{N,s} \text{P.V.} \int_{\mathbb{R}^N} \frac{u(x) - u(y)}{|x - y|^{N+2s}} dy$$

where $C_{N,s}$ is a normalization constant and P.V. denotes the Cauchy principle value. It is clear from the second definition that fractional Laplacian is a nonlocal operator, unlike the standard Laplacian. See [2] and [11] for rigorous definitions of both these operators.

Next, we discuss how to use fractional Laplacian as a regularizer in inverse problems arising in imaging science. In particular, we discuss image denoising problems. Recall that, typically one uses Total Variation (TV) seminorm as a regularizer in such settings [16]. Since fractional Laplacian enforces less smoothness and is a nonlocal operator, therefore it is excellent in capturing sharp transitions across interfaces. We establish that one can obtain comparable results using fractional Laplacian to TV and our proposed approach is significantly cheaper, one only needs to solve a linear equation instead of the nonlinear/degenerate problem in case of TV [1]. Notice that here one can simply define fractional Laplacian using periodic boundary conditions and can use Fast Fourier transform to solve the fractional PDE.

Next, we introduce yet another novel regularizer, i.e., a fractional operator where the fractional exponent is allowed to be spatially dependent, i.e., $s(x)$ instead of being a constant. Our approach is motivated the extension approach of [12, 17].

We allow the fractional exponent function to touch the extreme case of 0. We establish that, in this setting, we may not have density of smooth functions. We introduce novel function spaces and prove a trace theorem. Using this new operator as a regularizer in image denoising problems, we show that one can obtain almost perfect reconstructions which are significantly superior than TV based approaches [7].

Recall that, classical PDE based inverse problems are limited to identifying source/control located either on the boundary $\partial\Omega$ or in the interior of the domain Ω . However, with the help of fractional PDEs with integral fractional Laplacian, in [6, 8] we have introduced a completely new notion of inverse problems, i.e., the so-called external source/control problems.

We also discuss the notion of optimal control problems with semilinear fractional PDEs as constraints. Here we also allow control constraints. In the spectral case, we allow the control to be either in the interior or on the boundary [2]. In the integral case, the control is allowed to be in the interior [11] or in the exterior [6, 8]. We also present optimal control problems with fractional p -Laplacian (a quasilinear PDE) as constraints. The control here is given by the coefficient [10]. We also refer to [9] for results on state constrained problems.

In the last part of the talk we propose novel Deep Neural Networks (DNNs) derived using fractional time derivatives [5]. Fractional time derivatives are another class of nonlocal operators which have a distinct ability to capture memory effects. We first illustrate that the DNNs can be written as a constrained optimization problem. Next, we establish that fractional time derivatives, due to their nonlocal nature, can significantly help with the vanishing-gradient problem in DNNs. We conclude by illustrating the impact of fractional DNNs on Bayesian inverse problems.

REFERENCES

- [1] H. Antil and S. Bartels. *Spectral approximation of fractional PDEs in image processing and phase field modeling*, Comp. Meth. in Applied Mathematics **17**(4) (2017), 661–678.
- [2] H. Antil, J. Pfefferer, and S. Rogovs. *Fractional operators with inhomogeneous boundary conditions: Analysis, control, and discretization*, Commun. Math. Sci. **16**(5) (2018) 1395–1426.
- [3] H. Antil, Y. Chen, and A. Narayan. *Reduced basis methods for fractional Laplace equations via extension*, SIAM J. Sci. Comput. **41**(6) (2019), A3552–A3575.
- [4] H. Antil, D. Dondl, and L. Striet. *Approximation of Integral Fractional Laplacian and Fractional PDEs via sinc-Basis*, arXiv preprint arXiv:2010.06509 (2020).
- [5] H. Antil, R. Khatri, R. Löhner, and D. Verma. *Fractional deep neural network via constrained optimization*. Machine Learning: Science and Technology (2020).
- [6] H. Antil, R. Khatri and M. Warma. *External optimal control of nonlocal PDEs*, Inverse Problems **35**(8) 084003, 35.
- [7] H. Antil and C.N. Rautenberg. *Sobolev spaces with non-Muckenhoupt weights, fractional elliptic operators, and applications*, SIAM J. Math. Anal. **51**(3) (2019) 2479–2503.
- [8] H. Antil, D. Verma and M. Warma. *External optimal control of fractional parabolic PDEs*, ESAIM Control Optim. Calc. Var. **26** (2020).

- [9] H. Antil, D. Verma and M. Warma. *Optimal control of fractional elliptic PDEs with state constraints and characterization of the dual of fractional order sobolev spaces*, Journal of Optimization Theory and Applications (JOTA) (2020).
- [10] H. Antil and M. Warma. *Optimal control of the coefficient for the regional fractional p -Laplace equation: approximation and convergence*, **9**(1) (2019) 1–38.
- [11] H. Antil and M. Warma. *Optimal control of fractional semilinear PDEs*, ESAIM Control Optim. Calc. Var. **26** (2020).
- [12] L. Caffarelli and L. Silvestre. *An extension problem related to the fractional Laplacian*, Comm. Part. Diff. Eqs. **32**(7-9) (2007) 1245–1260.
- [13] A. Bonito and J.E. Pasciak. *Numerical approximation of fractional powers of elliptic operators*, Math. Comp. **84**(295) 2083–2110.
- [14] H. Dinh, and H. Antil, Y. Chen, E. Cherkaev, A. Narayan. *Model reduction for fractional elliptic problems using Kato’s formula*, arXiv preprint arXiv:1904.09332, (2019).
- [15] R.H. Nochetto, E. Otárola and A.J. Salgado. *A PDE Approach to Fractional Diffusion in General Domains: A Priori Error Analysis*, Found. Comput. Math. **15**(3) (2015) 733–791.
- [16] L.I. Rudin, S. Osher and E. Fatemi. *Nonlinear total variation based noise removal algorithms*, Physica D: nonlinear phenomena **60** (1992), 259–268.
- [17] P.R. Stinga and J.L. Torrea. *Extension problem and Harnack’s inequality for some fractional operators*, Comm. Part. Diff. Eqs. **35**(11) (2020) 2092–2122.
- [18] C.J. Weiss, B.G. van Bloemen Waanders, and H. Antil. *Fractional operators applied to geophysical electromagnetics*, Geophysical Journal International **220**(2) (2020), 1242–1259.

Analysis of a model of elastic dislocations in geophysics

ELENA BERETTA

(joint work with Andrea Aspri, Anna Mazzucato, Maarten de Hoop)

In my talk I analyse a mathematical model of *elastic dislocations* with applications to geophysics, where by elastic dislocation we mean an open, oriented Lipschitz surface in the interior of an elastic solid, across which there is a discontinuity of the displacement. I first briefly present the results in [1]; here we consider the case of the earth modelled as a inhomogeneous, isotropic elastic half-space and assume Lipschitz continuity of the elastic moduli and prove the existence and uniqueness of a very weak global solution to the forward problem of determining the displacement by imposing traction free boundary conditions at the surface of the earth, continuity of the traction and a given jump (slip-field) on the displacement across the fault.

Then I illustrate in details the results obtained in [2] for the case of discontinuous elastic moduli; the earth is a finite isotropic, inhomogeneous elastic layered medium (e.g. the earth) occupying a bounded region Ω in space, and the Lamé parameters are Lipschitz in each layer of the medium. In this case the displacement \mathbf{u} due to the slip-field \mathbf{g} acting on the dislocation (fault) S satisfies:

$$(1) \quad \begin{cases} \operatorname{div}(\mathbb{C}\widehat{\nabla}\mathbf{u}) = \mathbf{0}, & \text{in } \Omega \setminus \overline{S}, \\ (\mathbb{C}\widehat{\nabla}\mathbf{u})\boldsymbol{\nu} = \mathbf{0}, & \text{on } \Gamma_N, \\ \mathbf{u} = \mathbf{0}, & \text{on } \Gamma_D \\ [\mathbf{u}]_S = \mathbf{g}, \\ [(\mathbb{C}\widehat{\nabla}\mathbf{u})\mathbf{n}]_S = \mathbf{0}, \end{cases}$$

where \mathbb{C} is the piece-wise Lipschitz isotropic stiffness tensor and $\partial\Omega = \Gamma_D \cup \Gamma_N$.

I show existence of a unique variational solution to the forward problem assuming that the slip-field belongs to a suitable Sobolev trace space. I then use the well-posedness of the forward problem and the unique continuation property for solutions to the Lamé system, in the case of Lipschitz continuous parameters, to establish uniqueness in the inverse problem of determining the fault S and the displacement jump \mathbf{g} from measuring the displacement at the surface.

In the final part of my talk I describe some partial results obtained for the anisotropic case in the two-dimensional setting, [3], and some work in progress concerning a shape-derivative based algorithm for the reconstruction of a piece-wise linear dislocation from boundary measurements.

REFERENCES

- [1] A. Aspri, E. Beretta, A. Mazzucato, M. de Hoop, *Analysis of a model of elastic dislocations in geophysics*, Archive for Rational Mechanics and Analysis **236** (2020), 71-111.
- [2] A. Aspri, E. Beretta, A. Mazzucato, *Dislocations in a layered elastic medium with applications to fault detection* submitted, (2020), arXiv:2004.00321
- [3] A. Aspri, E. Beretta, M. de Hoop and A. Mazzucato, *Fault detection in an anisotropic elastic medium* submitted, (2020)

Where did the tumor start? Sparse reconstruction of initial conditions for reaction-diffusion PDEs

GEORGE BIROS

(joint work with Shashank Subramanian, Klaudius Scheufele, Miriam Mehl)

We present a numerical scheme for solving an inverse problem for parameter estimation in tumor growth models for glioblastomas, a form of aggressive primary brain tumor. The growth model is a reaction-diffusion partial differential equation (PDE) for the tumor concentration. We use a PDE-constrained optimization formulation for the inverse problem.

The unknown parameters are the reaction coefficient (proliferation), the diffusion coefficient (infiltration), and the initial condition field for the tumor PDE. Segmentation of Magnetic Resonance Imaging (MRI) scans from a single time snapshot drive the inverse problem where segmented tumor regions serve as partial observations of the tumor concentration. The precise time relative to tumor initiation is unknown, which poses an additional difficulty for inversion. We perform a frozen-coefficient spectral analysis and show that the inverse problem is

severely ill-posed. We introduce a biophysically motivated regularization on the tumor initial condition.

In particular, we assume that the tumor starts at a few locations (enforced with a sparsity constraint) and that the initial condition magnitude in the maximum norm equals one. We solve the resulting optimization problem using an inexact quasi-Newton method combined with a compressive sampling algorithm for the sparsity constraint. Our implementation uses PETSc and AccFFT libraries.

We conduct numerical experiments on synthetic and clinical images to highlight the improved performance of our solver over an existing solver that uses a two-norm regularization for the calibration parameters. The existing solver is unable to localize the initial condition. Our new solver can localize the initial condition and recover infiltration and proliferation. In clinical datasets (for which the ground truth is unknown), our solver results in qualitatively different solutions compared to the existing solver.

Bounds on Herglotz functions and physical limits to broadband passive cloaking in the quasistatic regime

MAXENCE CASSIER

(joint work with Graeme W. Milton)

Introduction: Cloaks are specific structures placed near or around an object that render the electromagnetic response of cloak plus object equal or almost equal to that of free space. Ideally passive cloaks should work for waves in a broadband frequency range, giving rise to the challenging question: Is it possible to perform broadband passive cloaking over a finite frequency band? In the context of the quasistatic approximation of Maxwell's equations we prove that it is impossible and give quantitative limitations to cloaking over a finite frequency range. Our results, published in [2], hold for a cloak or object of any geometrical shape and do not depend on the cloaking methods: transformation optics, anomalous resonance, complementary media.

1) *The passive cloaking problem.* Let \mathcal{O} be a bounded simply-connected dielectric inclusion with Lipschitz boundary that one wants to cloak. \mathcal{O} is characterized by its permittivity $\varepsilon(\mathbf{x}, \omega) = \varepsilon \mathbf{I}$, where $\varepsilon > \varepsilon_0$ is constant on the frequency range of interest $[\omega_-, \omega_+]$ and strictly larger than the permittivity of the vacuum ε_0 . The passive cloak is made of an anisotropic material of any shape characterized by its dielectric tensor $\varepsilon(\mathbf{x}, \omega)$ which depends both on the spatial variable \mathbf{x} and the frequency ω . The whole device, the inclusion and the cloak, occupies an open bounded set $\Omega \subset B(\mathbf{0}, R_0)$ of characteristic size R_0 and the remainder of space $\mathbb{R}^3 \setminus \Omega$ is vacuum of permittivity $\varepsilon(\mathbf{x}, \omega) = \varepsilon_0 \mathbf{I}$. The observer is assumed to be at a distance $R \gg R_0$.

We send a plane wave towards the device and assume that its wavelength is considerably larger than R in the frequency range of interest $\omega \in [\omega_-, \omega_+] \subset \mathbb{R}^{+,*}$ so that we can use the quasistatic approximation in this frequency band. In this

approximation, the curl-free electrical field $\mathbf{E}(\mathbf{x}, \omega)$ is given in terms of the gradient of some potential $V(\mathbf{x}, \omega)$, i.e. $\mathbf{E}(\mathbf{x}, \omega) = -\nabla V(\mathbf{x}, \omega)$, the incident plane wave in the vicinity of a closed ball $B(\mathbf{0}, R)$ corresponds to a uniform field $\mathbf{E}_0 \in \mathbb{C}^3$ so that the potential $\nabla V(\mathbf{x}, \omega)$ satisfies the following elliptic equation

$$(1) \quad \nabla \cdot (\boldsymbol{\varepsilon}(\mathbf{x}, \omega) \nabla V(\mathbf{x}, \omega)) = 0 \text{ on } \mathbb{R}^3,$$

and admits the asymptotic expansion as $|\mathbf{x}| \rightarrow \infty$:

$$(2) \quad V(\mathbf{x}, \omega) = -\mathbf{E}_0 \cdot \mathbf{x} + \frac{\mathbf{p}(\omega) \cdot \mathbf{x}}{4\pi\varepsilon_0|\mathbf{x}|^3} + \mathcal{O}\left(\frac{1}{|\mathbf{x}|^3}\right), \text{ with } \mathbf{p}(\omega) = \boldsymbol{\alpha}(\omega)\mathbf{E}_0.$$

Thus, the main contribution of the scattered far field is a dipolar term $\mathbf{p}(\omega) \in \mathbb{C}^3$ which depends linearly on \mathbf{E}_0 via the polarizability tensor $\boldsymbol{\alpha}(\omega) \in M_3(\mathbb{C})$. Hence, to cloak the device Ω at a sufficient large distance R to any incident field $\mathbf{E}_0 \in \mathbb{C}^3$ at a frequency $\omega \in [\omega_-, \omega_+]$, one needs that $\boldsymbol{\alpha}(\omega)$ vanishes at ω .

The electric induction \mathbf{D} is given within the cloak $\Omega \setminus \mathcal{O}$ by the constitutive law (CL): $\mathbf{D} = \varepsilon_0 \mathbf{E} + \varepsilon_0 \boldsymbol{\chi}_E \star_t \mathbf{E}$, where \star_t stands for the time convolution product between the real-valued susceptibility tensor $\boldsymbol{\chi}_E(\mathbf{x}, t)$ and the electrical field \mathbf{E} . To define this convolution, one assumes for simplicity that $\boldsymbol{\chi}_E \in L^1(\mathbb{R}_t, L^\infty(\Omega \setminus \mathcal{O})^9)$ and that $\mathbf{E}, \partial_t \mathbf{E} \in L^2(\mathbb{R}_t, L^2(\Omega \setminus \mathcal{O})^3)$. The cloak is a passive material since **it is causal**: $\boldsymbol{\chi}_E$ is supported in $(\Omega \setminus \mathcal{O}) \times \mathbb{R}_t^+$ and **passive**, i.e. for any real fields (\mathbf{E}, \mathbf{D}) satisfying the (CL) (and the regularity assumptions for \mathbf{E}):

$$\int_{-\infty}^t \int_{\Omega \setminus \mathcal{O}} \partial_t \mathbf{D}(\mathbf{x}, t) \cdot \mathbf{E}(\mathbf{x}, t) d\mathbf{x} dt \geq 0, \quad \forall t \in \mathbb{R}.$$

Let $\mathbb{C}^+ := \{\omega \in \mathbb{C} \mid \text{Im } \omega > 0\}$ and $\text{cl } \mathbb{C}^+ := \mathbb{C}^+ \cup \mathbb{R}$. For any causal $f \in L^1(\mathbb{R}_t)$, one defines the Fourier-Laplace transform as $\hat{f}(\omega) := \int_{\mathbb{R}_+} f(t) e^{i\omega t} dt$, $\forall \omega \in \text{cl } \mathbb{C}^+$ so that it coincides with the Fourier transform for real frequency. The (CL) in the frequency domain becomes: $\hat{\mathbf{D}}(\mathbf{x}, \omega) = \boldsymbol{\varepsilon}(\mathbf{x}, \omega) \hat{\mathbf{E}}(\mathbf{x}, \omega)$ with $\boldsymbol{\varepsilon}(\mathbf{x}, \omega) = \varepsilon_0(1 + \hat{\boldsymbol{\chi}}_E(\mathbf{x}, \omega))$, $\forall \omega \in \mathbb{R}$. Thus, one shows that the passivity of the cloak is equivalent in the frequency domain to

($\tilde{\text{H}}_1$): for a.e. $\mathbf{x} \in \Omega \setminus \mathcal{O}$, $\boldsymbol{\varepsilon}(\mathbf{x}, \cdot)$ is analytic on \mathbb{C}^+ and continuous on $\text{cl } \mathbb{C}^+$,

($\tilde{\text{H}}_2$): for a.e. $\mathbf{x} \in \Omega \setminus \mathcal{O}$, $\forall \omega \in \text{cl } \mathbb{C}^+$, $\boldsymbol{\varepsilon}(\mathbf{x}, -\bar{\omega}) = \overline{\boldsymbol{\varepsilon}(\mathbf{x}, \omega)}$,

($\tilde{\text{H}}_3$): for a.e. $\mathbf{x} \in \Omega \setminus \mathcal{O}$, $\forall \omega \in \mathbb{R}^+$, $\text{Im } \boldsymbol{\varepsilon}(\mathbf{x}, \omega) \geq 0$ (passivity),

($\tilde{\text{H}}_4$): for a.e. $\mathbf{x} \in \Omega \setminus \mathcal{O}$, $\boldsymbol{\varepsilon}(\mathbf{x}, \omega) \rightarrow \varepsilon_0 \mathbf{I}$ as $|\omega| \rightarrow \infty$ in $\text{cl } \mathbb{C}^+$.

2) *Bounds on Herglotz functions and passive systems.* Herglotz functions are analytic functions of the upper-half plane with non-negative imaginary part. In [2], we derive bounds on Herglotz functions which apply to a wide class of linear passive systems and generalize those provided in [1]. To this aim, we consider a passive linear system characterized by a function $f : \text{cl } \mathbb{C}^+ \rightarrow \mathbb{C}$ in the frequency domain which satisfies the assumptions

(H_1) f is analytic on \mathbb{C}^+ , continuous on $\text{cl } \mathbb{C}^+$, (H_2) $f(-\bar{\omega}) = \overline{f(\omega)}$, $\forall \omega \in \text{cl } \mathbb{C}^+$,

(H_3) $\text{Im } f(\omega) \geq 0$, $\forall \omega \in \mathbb{R}^+$, (H_4) $f(\omega) \rightarrow f_\infty > 0$, when $|\omega| \rightarrow \infty$ in $\text{cl } \mathbb{C}^+$,

i.e. ($\tilde{\text{H}}_1 - \tilde{\text{H}}_4$) but for a scalar function. We define the square root by $\sqrt{\omega} =$

$|\omega|^{\frac{1}{2}} e^{i \arg \omega / 2}$ if $\arg \omega \in (0, 2\pi)$ and by $\sqrt{x} = |x|^{\frac{1}{2}}$ for $x \in \mathbb{R}^+$. In [2], we show that v defined by $v(\omega) := \omega f(\sqrt{\omega})$, $\forall \omega \in \mathbb{C}$ is a Herglotz function that is analytic in $\mathbb{C} \setminus \mathbb{R}^+$, negative on $\mathbb{R}^{-,*}$ and satisfies by (H₂): $v(\overline{\omega}) = \overline{v(\omega)}$, $\forall \omega \in \mathbb{C}^+ \cup \mathbb{R}^{-,*}$ and by (H₄): $v(\omega) = f_\infty \omega + o(\omega)$ when $|\omega| \rightarrow \infty$ in \mathbb{C}^+ .

Then, we introduce the Herglotz functions h_m and v_m defined by:

$$h_m(\omega) = \int_{\mathbb{R}} \frac{dm(\xi)}{\xi - \omega} \quad \text{and} \quad v_m(\omega) = h_m(v(\omega)), \quad \forall \omega \in \mathbb{C}^+,$$

where $m \in \mathcal{M}$ with \mathcal{M} is the set of probability measures on \mathbb{R} . Using a sum rule derived in [1], we show (see [2]) the following theorem.

Theorem 1. *Let $[x_-, x_+]$ be a compact interval of $\mathbb{R}^{+,*}$, then one has:*

$$(3) \quad \lim_{y \rightarrow 0^+} \frac{1}{\pi} \int_{x_-}^{x_+} \text{Im } v_m(x + iy) dx \leq \frac{1}{f_\infty} \quad \forall m \in \mathcal{M},$$

and Dirac measures $(\delta_\xi)_{\xi \in \mathbb{R}}$ optimize the inequality (3) since

$$\sup_{m \in \mathcal{M}} \frac{1}{\pi} \lim_{y \rightarrow 0^+} \int_{x_-}^{x_+} \text{Im } v_m(x + iy) dx = \sup_{\xi \in \mathbb{R}} \frac{1}{\pi} \lim_{y \rightarrow 0^+} \int_{x_-}^{x_+} \text{Im } v_{\delta_\xi}(x + iy) dx.$$

We prove this result in [2] for compactly supported measures $m \in \mathcal{M}$ but it can be shown exactly in the same way for any $m \in \mathcal{M}$. If $\text{Im } f(\omega) = 0$ for $\omega \in [\omega_-, \omega_+]$, we show by using Dirac measures $(\delta_\xi)_{\xi \in \mathbb{R}}$ in inequality (3) that

$$(4) \quad \omega_0^2 (f(\omega_0) - f_\infty) \leq \omega^2 (f(\omega) - f_\infty), \quad \forall \omega, \omega_0 \in [\omega_-, \omega_+] \text{ such that } \omega_0 \leq \omega.$$

Without such assumption on $\text{Im } f$, by using the uniform probability measure on $[-\Delta, \Delta]$ with $\Delta = \max_{[\omega_-, \omega_+]} |v(x)|$ in the bound (3) it follows that:

$$(5) \quad \frac{1}{4} (\omega_+^2 - \omega_-^2) f_\infty \leq \max_{\omega \in [\omega_-, \omega_+]} |\omega^2 f(\omega)|.$$

3) *Fundamentals limits to broadband cloaking.* We apply now the above bounds to cloaking. We give in [2] a functional framework to equations (1) and (2) (which are physically relevant in $[\omega_-, \omega_+]$ where the quasistatic approximation is valid but holds for any $\omega \in \text{cl } \mathbb{C}^+$ by using the analytic extension of the permittivity in the inclusion and in the vacuum). Then, we show (with a coercivity assumption, see [2]) that for a passive cloak satisfying $(\tilde{H}_1 - \tilde{H}_4)$ and a reciprocity principle, the function $f_{\mathbf{E}_0}$ given by

$$f_{\mathbf{E}_0}(\omega) := \boldsymbol{\alpha}(\omega) \mathbf{E}_0 \cdot \overline{\mathbf{E}_0} = \int_{\Omega} (\boldsymbol{\varepsilon}(\mathbf{x}, \omega) - \varepsilon_0 \mathbf{I}) \mathbf{E}(\mathbf{x}, \omega) \cdot \overline{\mathbf{E}_0} d\mathbf{x}, \quad \forall \omega \in \text{cl } \mathbb{C}^+$$

is well-defined for $\mathbf{E}_0 \in \mathbb{C}^3$ and satisfies $(\tilde{H}_1 - \tilde{H}_4)$ with $f_{\mathbf{E}_0, \infty} := \boldsymbol{\alpha}(\infty) \mathbf{E}_0 \cdot \overline{\mathbf{E}_0}$ where $\boldsymbol{\alpha}(\infty) := \lim_{|\omega| \rightarrow +\infty} \boldsymbol{\alpha}(\omega)$ is the positive definite polarizability tensor of the inclusion \mathcal{O} depending only on its geometry and contrast in permittivity. If the cloak is a lossless (i.e if $\text{Im } \boldsymbol{\varepsilon}(\mathbf{x}, \omega) = 0$ inside the cloak on $[\omega_-, \omega_+]$), one shows that $\text{Im } f_{\mathbf{E}_0}(\omega) = 0$ on $[\omega_-, \omega_+]$. Thus, using (4) on functions $f_{\mathbf{E}_0}$ gives

$$\omega_0^2 (\boldsymbol{\alpha}(\omega_0) - \boldsymbol{\alpha}(\infty)) \leq \omega^2 (\boldsymbol{\alpha}(\omega) - \boldsymbol{\alpha}(\infty)), \quad \forall \omega, \omega_0 \in [\omega_-, \omega_+] \text{ such that } \omega_0 \leq \omega,$$

which turns to be an optimal bound (see [2]). Now assume that one can cloak at

a frequency ω_0 . Thus $\alpha(\omega_0) = 0$ and it yields to

$$\alpha(\omega) \leq -\alpha(\infty) \frac{\omega_0^2 - \omega^2}{\omega^2}, \quad \omega \in [\omega_-, \omega_0] \quad \text{and} \quad \alpha(\infty) \frac{\omega^2 - \omega_0^2}{\omega^2} \leq \alpha(\omega), \quad \omega \in [\omega_0, \omega_+]$$

which obviously forces $\alpha(\omega)$ to be non-zero away from the frequency ω_0 on $[\omega_-, \omega_+]$ and makes cloaking impossible on $[\omega_-, \omega_+]$. If the cloak is not lossless, one applies the bound (5) on the functions $f_{\mathbf{E}_0}$ to get:

$$\frac{1}{4}(\omega_+^2 - \omega_-^2)\alpha(\infty)\mathbf{E}_0 \cdot \overline{\mathbf{E}_0} \leq \max_{\omega \in [\omega_-, \omega_+]} |\omega^2 \alpha(\omega) \mathbf{E}_0 \cdot \overline{\mathbf{E}_0}|, \quad \forall \mathbf{E}_0 \in \mathbb{C}^3.$$

This positive lower bound also gives a limitation to cloaking on $[\omega_-, \omega_+]$.

REFERENCES

- [1] A. Bernland, A. Luger, and M. Gustafsson, *Sum rules and constraints on passive systems*, J. Phys. A Math. Theor., **44**(14) (2011), 145205.
- [2] M. Cassier and G. W. Milton, *Bounds on Herglotz functions and fundamental limits of broadband passive quasistatic cloaking*, J. Math. Phys., **58**(7) (2017), 071504.

On model reduction for tomographic inverse problems

HERBERT EGGER

(joint work with Jürgen Dölz, Matthias Schlottbom)

Tomographic applications typically involve measurements for multiple excitations and detectors which can be interpreted as finite dimensional projections of infinite dimensional measurement operators. The corresponding inverse problems can then be phrased as ill-posed linear operator equations

$$(1) \quad \mathcal{T}(c) = \mathcal{M}^\delta$$

with c denoting the unknown field to be determined and \mathcal{M}^δ representing a perturbed version of the complete measurement operator. In typical applications, like inverse scattering or optical tomography, the forward operator or its linearization has a canonical factorization [5]

$$(2) \quad \mathcal{T}(c) = \mathcal{V}^* \mathcal{D}(c) \mathcal{U}$$

with operators \mathcal{U} and \mathcal{V} representing excitation or detectors fields and $\mathcal{D}(c)$ describing the interaction with the medium to be probed. This factorization reveals the tensor product structure of the forward operator $\mathcal{T}(c)$.

After discretization, the forward operator can be interpreted as a high-dimensional mapping $\mathcal{T} : \mathbb{R}^m \rightarrow \mathbb{R}^{k \times k}$, with m denoting the number of parameters to be determined, and k the number of excitations and detectors. A single evaluation of the forward operator $\mathcal{T}(c)$ may then already have a very high complexity $O(mk^2)$ and some model reduction or low-rank approximation is required for an efficient solution of the inverse problem.

For any given accuracy, the low-rank approximation of minimal rank is given by the truncated singular value decomposition [4] which, however, will in general not have a tensor-product form. As a consequence, even for approximations generated by stochastic algorithms [8], the setup and memory cost of the TSVD is usually too

high for practical purposes. Alternative low-rank approximations, explicitly taking account of the underlying tensor-product structure, have been investigated in [1, 6, 7]. While these approaches reduce the computational complexity of the setup and memory cost, the rank of the resulting approximations is usually much higher than that of the corresponding TSVD, and the solution of the inverse problem remains computationally demanding.

In this talk, we present a strategy that is based on an intermediate sparse tensor-product approximation [3] and a sub-sequent truncated singular value decomposition. This allows us to generate an approximation $\mathcal{T}_N(x) = \mathcal{Q}_N \mathcal{T}(c)$ of the forward operator via an orthogonal projection \mathcal{Q}_N in data space with quasi-optimal rank for a given accuracy but at a computational cost which essentially amounts to that of a single evaluation $\mathcal{T}(c)$ of the full forward operator. A rigorous analysis is given in [2]. After setup of the low-rank approximation \mathcal{T}_N for the forward operator, the regularized solution of the inverse problem can be executed very efficiently in a three step procedure

$$\begin{aligned} \mathcal{M}_N^\delta &= \mathcal{Q}_N \mathcal{M}^\delta && \text{(data compression)} \\ z_{\alpha,N}^\delta &= g_\alpha(\mathcal{T}\mathcal{T}^*) \mathcal{M}_N^\delta && \text{(regularized inversion)} \\ c_{\alpha,N}^\delta &= \mathcal{T}^* z_{\alpha,N}^\delta && \text{(back projection)} \end{aligned}$$

Note that the regularized inversion now only depends on the dimension N of the low-rank approximation can therefore be computed extremely efficient. Assuming that the dimension $k \times k$ of the full data \mathcal{M}^δ is larger then the dimension m of the parameter c to be determined, the data compression step turns out to be of the highest computational complexity. Using the underlying sparse tensor-product structure of \mathcal{Q}_N , this step can still be computed rather efficiently and in a way such that access to the full data \mathcal{M}^δ is never required.

REFERENCES

- [1] S. Chaillat and G. Biros, *FaIMS: A fast algorithm for the inverse medium problem with multiple frequencies and multiple sources for the scalar Helmholtz equation*, J. Comput. Phys., 231 (2012), 4403–4421.
- [2] J. Dölz, H. Egger, and M. Schlottbom, *A model reduction approach for inverse problems with operator valued data*, arXiv:2004.11827, 2020.
- [3] D. Düng, V. Temlyakov, and T. Ullrich, *Hyperbolic cross approximation*, Birkhäuser/Springer, Cham, 2018.
- [4] G. H. Golub and C. F. Van Loan, *Matrix computations. 4th ed.*, Johns Hopkins University Press, Baltimore, MD, 2013.
- [5] N. Grinberg and A. Kirsch, *The Factorization Method for Inverse Problems*, vol. 36 of Oxford Lecture Series in Mathematics and its Applications, Oxford University Press, New York, 2008.
- [6] J. R. Krebs, J. E. Anderson, D. Hinkley, R. Neelamani, S. Lee, A. Baumstein, and M.-D. Lacasse, *Fast full-wavefield seismic inversion using encoded sources*, Geophysics, 74 (2009), WCC177–WCC188.
- [7] V. A. Markel, H. Levinson, and J. C. Schotland, *Fast linear inversion for highly overdetermined inverse scattering problems*, Inverse Problems, 35 (2019), 124002.
- [8] F. Roosta-Khorasani, K. van den Doel, and U. Ascher, *Stochastic algorithms for inverse problems involving PDEs and many measurements*, SIAM Journal on Scientific Computing, 36 (2014), S3–S22.

**Wave Propagation and Correlation-based Imaging in Random Media:
From Gaussian to non-Gaussian Statistics**

JOSSELIN GARNIER

In this talk we consider wave propagation in random open media and in random open waveguides. In both cases an asymptotic analysis based on a separation of scales technique [3] makes it possible to compute the statistics of the wave field and to design imaging algorithms based on the empirical cross correlations of the recorded signals.

In random open media the wave field can be characterized in the random paraxial regime, when the wavelength is smaller than the correlation length of the medium and the beam radius, which are themselves smaller than the typical propagation distance [6]. The mean or coherent wave decays exponentially with the propagation distance and the mean Wigner transform (the partial Fourier transform of the two-point covariance function of the wave field) satisfies a radiative transfer equation. The fourth-order moment analysis [7] also reveals that the statistics of the wave field behaves as a Gaussian process, in the sense that the fourth-order moments satisfy the Isserlis formula and the scintillation index (the relative variance of the intensity) goes to one for large propagation distances.

In random open waveguides, the wave field can be expanded on the complete set of the modes of the unperturbed waveguide. When random perturbations affect the index of refraction within the core of the waveguide or the geometry of the core boundary, the mean guided mode amplitudes decay exponentially and the mean guided mode powers satisfy a coupled mode equation, which can be interpreted as a discrete form of the radiative transfer equation [1, 5]. The coupling between guided and radiating modes also induces effective losses for the mean guided mode powers [4]. The fourth-order moment analysis reveals that the fluctuations of the guided mode powers grow exponentially with the propagation distance [4]. This is, therefore, in contrast with the situation in open random medium. By studying the exponential growth rates of the relative variances of the guided mode powers, it is possible to show that, when the number of guided modes increases, the exponential growth rates vanish and the scintillation index becomes equal to one [4], as observed in open medium in the random paraxial regime [7].

These results show that incoherent imaging in a random open waveguide, such as a Pekeris waveguide in underwater acoustics, is challenging when the number of propagating modes is not large. Indeed incoherent imaging is based on the use of the cross correlations of the recorded signals. The estimation of the second-order moments of the wave field is, however, difficult because of the large variances of the empirical second-order moments and one may need to average over a lot a samples, while the medium may be not stationary as in underwater acoustics. This is in contrast with the situation in open random media where smoothed Wigner transforms are statistically stable [7]. It is, however, possible to extract some limited information about the environment from the cross correlations of the recorded signals in random open waveguides by Bayesian inference [2].

More generally, the results on the fourth-order moments show that the predictions of the coupled mode equations, which describe the evolutions of the statistical second-order moments of the wave field, are not easy to exploit experimentally in random open waveguides when the number of guided modes is not large. The situation is easier in random closed waveguides because of the absence of radiating modes.

REFERENCES

- [1] R. Alonso, L. Borcea, and J. Garnier, *Wave propagation in waveguides with rough boundaries*, Commun. Math. Sci. **11** (2012), 233–267.
- [2] L. Dumaz, J. Garnier, and G. Lepoutier, *Acoustic and geoacoustic inverse problems in randomly perturbed shallow-water environments*, J. Acoust. Soc. Am. **146** (2019), 458–469.
- [3] J.-P. Fouque, J. Garnier, G. Papanicolaou, and K. Sølna, *Wave Propagation and Time Reversal in Randomly Layered Media*, Springer, New York, 2007.
- [4] J. Garnier, *Intensity fluctuations in random waveguides*, Commun. Math. Sci. **18** (2020), 947–971.
- [5] J. Garnier and G. Papanicolaou, *Pulse propagation and time reversal in random waveguides*, SIAM J. Appl. Math. **67** (2007), 1718–1739.
- [6] J. Garnier and K. Sølna, *Coupled paraxial wave equations in random media in the white-noise regime*, Ann. Appl. Probab. **19** (2009), 318–346.
- [7] J. Garnier and K. Sølna, *Fourth-moment analysis for beam propagation in the white-noise paraxial regime*, Arch. Ration. Mech. Anal. **220** (2016), 37–81.

Deep learning architectures for nonlinear operator functions and nonlinear inverse problems

MAARTEN V. DE HOOP

(joint work with Matti Lassas, Christopher A. Wong)

We develop a theoretical analysis for special neural network architectures, termed operator recurrent neural networks, for approximating highly nonlinear functions whose inputs are linear operators. Such functions commonly arise in solution algorithms for inverse problems for the wave equation. Traditional neural networks treat input data as vectors, and thus they do not effectively capture the multiplicative structure associated with the linear operators that correspond to the measurement data in such inverse problems. We therefore introduce a new parametric family that resembles a standard neural network architecture, but where the input data acts multiplicatively on vectors.

Motivated by compact operators appearing in boundary control and the analysis of inverse boundary value problems for the wave equation, we promote structure and sparsity in selected weight matrices in the network. After describing this architecture, we study its representation properties as well as its approximation properties. We furthermore show that an explicit regularization can be introduced that can be derived from the mathematical analysis of the mentioned inverse problems, and which leads to some guarantees on the generalization properties. We observe that the sparsity of the weight matrices improves the generalization estimates. Lastly, we discuss how operator recurrent networks can be viewed as a deep

learning analogue to deterministic algorithms such as boundary control for reconstructing the unknown wavespeed in the acoustic wave equation from boundary measurements.

Numerical analysis of diffusion coefficient identification for elliptic and parabolic systems

BANGTI JIN

(joint work with Zhi Zhou)

Parameter identifications for differential equations represent a wide class of inverse problems. Many deep results on conditional stability have been established for concrete parameter identification problems. Meanwhile, a large variety of inversion schemes have been proposed, often based on Tikhonov regularization. Thus, it is natural to ask whether one can use conditional stability results to analyze relevant numerical procedures. Conditional stability has been employed to derive convergence rates for Tikhonov regularization in [2]. However, it has not been employed to analyze discrete schemes.

In this work, we make an attempt to exploit “stability” results for deriving convergence rates for a discrete scheme for recovering a spatially dependent diffusion coefficient q in an elliptic or parabolic type problem. Let $\Omega \subset \mathbb{R}^d$ ($d = 1, 2, 3$) be a convex polyhedral domain with a boundary $\partial\Omega$. Consider the following elliptic problem:

$$(1) \quad \begin{cases} -\nabla \cdot (q\nabla u) = f, & \text{in } \Omega, \\ u = 0, & \text{on } \partial\Omega, \end{cases}$$

where the function f denotes a given source term. The solution to problem (1) is denoted by $u(q)$. The inverse problem is to recover the exact diffusion coefficient q^\dagger from the pointwise observation z^δ , with a noise level δ , $\|z^\delta - u(q^\dagger)\|_{L^2(\Omega)} \leq \delta$. The diffusion coefficient q is assumed to satisfy $0 < c_0 \leq q \leq c_1$ in Ω . Problem (1) is the steady state of the following parabolic type problem

$$(2) \quad \begin{cases} \partial_t^\alpha u - \nabla \cdot (q\nabla u) = f, & \text{in } \Omega \times (0, T], \\ u(0) = u_0, & \text{in } \Omega, \\ u = 0, & \text{on } \partial\Omega \times (0, T], \end{cases}$$

where $T > 0$ is the final time, and $0 < \alpha \leq 1$. The functions f and u_0 are the given source term and initial condition, respectively. The notation $\partial_t^\alpha u$ denotes the Djrbashian-Caputo fractional derivative of order $\alpha \in (0, 1)$, defined by

$$\partial_t^\alpha u(t) = \frac{1}{\Gamma(1-\alpha)} \int_0^t (t-s)^{-\alpha} u'(s) ds,$$

where $\Gamma(z)$ denotes Euler’s Gamma function. For $\alpha = 1$, it coincides with the usual first-order derivative. In this case, the inverse problem is to recover the spatially dependent diffusion coefficient q^\dagger from the distributed observation z^δ over $\Omega \times (0, T)$, with a noise level δ , i.e., $\|z^\delta - u(q^\dagger)\|_{L^2(0,T;L^2(\Omega))} \leq \delta$. Problems

(1) and (2) describe many important physical processes, and for $0 < \alpha < 1$, the model describes the so-called subdiffusion process.

Now we describe one inversion scheme based on Tikhonov regularization and Galerkin FEM approximation. Let \mathcal{T}_h be a shape regular quasi-uniform triangulation of the domain Ω into d -simplexes with a mesh size h . Over \mathcal{T}_h , we define two finite element spaces: $X_h = \{v_h \in H_0^1(\Omega) : v_h|_K \in P_1(K) \forall K \in \mathcal{T}_h\}$ and $V_h = \{v_h \in H^1(\Omega) : v_h|_K \in P_1(K) \forall K \in \mathcal{T}_h\}$, which are used to approximate the state u and the diffusion coefficient q , respectively. Now the inversion scheme for problem (1) reads

$$(3) \quad \min_{q_h \in \mathcal{A}_h} J_{\gamma,h}(q_h) = \frac{1}{2} \|u_h(q_h) - z^\delta\|_{L^2(\Omega)}^2 + \frac{\gamma}{2} \|\nabla q_h\|_{L^2(\Omega)}^2,$$

with $\mathcal{A}_h = \{q_h \in V_h : c_0 \leq q_h(x) \leq c_1 \text{ in } \Omega\}$ and $u_h(q_h)$ satisfying

$$(4) \quad (q_h \nabla u_h(q_h), \nabla v_h) = (f, v_h), \quad \forall v_h \in X_h.$$

Then in the work [4], the following weighted error estimate was proved using an energy argument, with a novel test function.

Theorem 1 (Elliptic case). *Let the exact diffusion coefficient $q^\dagger \in H^2(\Omega) \cap W^{1,\infty}(\Omega)$, $u(q^\dagger)$ the solution to problem (1) with $f \in L^\infty(\Omega)$, and $q_h^* \in \mathcal{A}_h$ a minimizer of problem (3)-(4). Then with $\eta = h^2 + \delta + \gamma^{\frac{1}{2}}$, there holds*

$$\int_{\Omega} (q^\dagger - q_h^*)^2 (q^\dagger |\nabla u(q^\dagger)|^2 + fu(q^\dagger)) \, dx \leq c(h\gamma^{-\frac{1}{2}}\eta + \min(h + h^{-1}\eta, 1))\gamma^{-\frac{1}{2}}\eta.$$

Theorem 1 allows deriving the standard $L^2(\Omega)$ bound, under condition (5), which holds for certain problem data [1].

Corollary 1. *Let $q^\dagger \in H^2(\Omega) \cap W^{1,\infty}(\Omega)$ and $f \in L^\infty(\Omega)$, and assume that there exists some $\beta \geq 0$ such that*

$$(5) \quad (q^\dagger |\nabla u(q^\dagger)|^2 + fu(q^\dagger))(x) \geq c \text{dist}(x, \partial\Omega)^\beta \quad \text{a.e. in } \Omega.$$

Then the approximation q_h^ satisfies*

$$\|q^\dagger - q_h^*\|_{L^2(\Omega)} \leq c((h\gamma^{-\frac{1}{2}}\eta + \min(h^{-1}\eta, 1))\gamma^{-\frac{1}{2}}\eta)^{\frac{1}{2(1+\beta)}}.$$

For any $\delta > 0$, the choices $\gamma \sim \delta^2$ and $h \sim \sqrt{\delta}$ imply $\|q^\dagger - q_h^\|_{L^2(\Omega)} \leq c\delta^{\frac{1}{4(1+\beta)}}$.*

To discretize problem (2), we divide the time interval $[0, T]$ uniformly, with grid points $t_n = n\tau$, $n = 0, \dots, N$, and a time step size $\tau = T/N$, and then employ the standard Galerkin finite element method in space and backward Euler convolution quadrature in time. The latter, denoted by $\bar{\partial}_\tau^\alpha \varphi^n$ (with $\varphi^j = \varphi(t_j)$), is defined by [3]:

$$\bar{\partial}_\tau^\alpha \varphi^n = \tau^{-\alpha} \sum_{j=0}^n b_j^{(\alpha)} \varphi^{n-j}, \quad \text{with } (1 - \xi)^\alpha = \sum_{j=0}^\infty b_j^{(\alpha)} \xi^j.$$

Then the inversion scheme in the parabolic case reads

$$(6) \quad \min_{q_h \in \mathcal{A}_h} J_{\gamma,h,\tau}(q_h) = \frac{\tau}{2} \sum_{n=1}^N \|U_h^n(q_h) - z_n^\delta\|_{L^2(\Omega)}^2 + \frac{\gamma}{2} \|\nabla q_h\|_{L^2(\Omega)}^2,$$

with $z_n^\delta = \tau^{-1} \int_{t_{n-1}}^{t_n} z^\delta dt$, and $U_h^n(q_h) \in X_h$ satisfying $U_h^0(q_h) = P_h u_0$ and

$$(7) \quad (\bar{\partial}_\tau^\alpha (U_h^n - U_h^0), \chi) + (q \nabla U_h^n, \nabla \chi) = (f^n, \chi), \quad \forall \chi \in X_h, \quad n = 1, 2, \dots, N,$$

with $f^n = \frac{1}{\tau} \int_{t_{n-1}}^{t_n} f(s) ds$.

Then the following error estimate holds for the standard parabolic case [4]; see also [5] for the case $0 < \alpha < 1$. Just as in the elliptic case, a similar positivity condition can be verified to derive the standard $L^2(\Omega)$ bound.

Theorem 2 (Standard parabolic case). *Let $q^\dagger \in H^2(\Omega) \cap W^{1,\infty}(\Omega)$, $u_0 \in H^2(\Omega) \cap H_0^1(\Omega) \cap W^{1,\infty}(\Omega)$, and $f \in L^\infty((0, T) \times \Omega) \cap C^1([0, T]; L^2(\Omega)) \cap W^{2,1}(0, T; L^2(\Omega))$. Let $q_h^* \in \mathcal{A}_h$ be a solution to problem (6)–(7). Then with $\eta = \tau + h^2 + \delta + \gamma^{\frac{1}{2}}$, there holds*

$$\begin{aligned} & \tau^3 \sum_{j=1}^N \sum_{i=1}^j \sum_{n=i}^j \int_{\Omega} \left(\frac{q^\dagger - q_h^*}{q^\dagger} \right)^2 \left(q^\dagger |\nabla u(t_n)|^2 + (f(t_n) - \partial_t u(t_n)) u(t_n) \right) dx \\ & \leq c(h\gamma^{-\frac{1}{2}}\eta + \min(1, h^{-1}\eta))\gamma^{-\frac{1}{2}}\eta. \end{aligned}$$

One- and two-dimensional numerical experiments show that a steady convergence can be observed, but the theoretical prediction remains suboptimal. The optimal rates remain to be established.

REFERENCES

- [1] A. Bonito, A. Cohen, R. DeVore, G. Petrova, G. Welper, *Diffusion coefficients estimation for elliptic partial differential equations*, SIAM J. Math. Anal. **49** (2017), 1570–1592.
- [2] J. Cheng, M. Yamamoto, *One new strategy for a priori choice of regularizing parameters in Tikhonov's regularization*, Inverse Problems **16** (2000), L31–L38.
- [3] B. Jin, R. Lazarov, Z. Zhou, *Two fully discrete schemes for fractional diffusion and diffusion-wave equations with nonsmooth data*, SIAM J. Sci. Comput. **38** (2016), A146–A170.
- [4] B. Jin, Z. Zhou, *Error analysis of finite element approximations of diffusion coefficient identification for elliptic and parabolic problems*, SIAM J. Numer. Anal., 2020, in press.
- [5] B. Jin, Z. Zhou, *Numerical estimation of a diffusion coefficient in subdiffusion*, Preprint, arXiv:1909.00334.

Simulation of non-linear magnetization effects and parameter identification problems in magnetic particle imaging

TOBIAS KLUTH

(joint work with Hannes Albers)

Magnetic particle imaging (MPI) is an emerging imaging modality exploiting the magnetization behavior of nanoparticles in a highly dynamic applied magnetic field (see [4] for a comprehensive review on MPI methodology). A proper solution to the imaging problem, i.e., the reconstruction of a space- and potentially time-dependent concentration function, requires an adequate solution to the calibration problem, i.e., a proper model and parameters therein for the mean magnetic moment $\bar{\mathbf{m}}$ of an ensemble of nanoparticles. Finding a suitable solution to the

model-based calibration problem is one of the open challenges in MPI such that a fully measured approach is still the state of the art.

The dynamic behavior of the nanoparticles' magnetic moments is affected by Brownian and Néel mechanisms. The former describes the magnetic moment rotation due to rotation of the whole particle while the later describes the internal rotation of the magnetic moment (see, e.g., [2] for details in the context of MPI). Both of these magnetic moment dynamics can be modeled individually in an effective manner for large ensembles of nanoparticles using the Fokker-Planck equation to reformulate the stochastic ODE into a deterministic PDE whose solution is the probability density over all magnetic moment directions (for a detailed derivation, see [2]). In particular, we obtain an advection-diffusion equation on the sphere S^2 for the probability density function (pdf) $f : S^2 \times I \times \Omega \rightarrow \mathbb{R}_+ \cup \{0\}$ (measurement time interval $I = [0, T] \subset \mathbb{R}$, field-of-view $\Omega \subset \mathbb{R}^3$):

$$\frac{\partial}{\partial t} f = \operatorname{div}_{S^2} \left(\frac{1}{2\tau} \nabla_{S^2} f - \mathbf{b}(\cdot, \mathbf{H} + \delta \mathbf{h}) f \right)$$

with relaxation time constant $\tau > 0$, applied magnetic field $\mathbf{H} : I \times \Omega \rightarrow \mathbb{R}^3$, and the (velocity) field $\mathbf{b} : S^2 \times \mathbb{R}^3 \rightarrow \mathbb{R}^3$ given by

$$\mathbf{b}(m, h) = p_1 h \times m + p_2 (m \times h) \times m$$

for $p_i \geq 0$, $i = 1, 2$. The domain of $\delta \mathbf{h}$ may differ depending on the modeling of particle behavior, e.g., in the case of uniaxial anisotropy with $\delta \mathbf{h} : S^2 \rightarrow \mathbb{R}^3$, $\delta \mathbf{h}(m) = p_3 (m \cdot n) n$ for an easy axis $n \in S^2$ and $p_3 > 0$. The choice of parameters $(p_i)_i$ depends on the chosen rotation model and physical properties of the tracer material. These scalar parameters may only be known approximately in practice; thus it may be advantageous to include their identification in the parameter identification scheme described in the following. Once the Fokker-Planck equation has been solved, the desired mean magnetic moment can be obtained in a straightforward manner by taking the mean of the resulting pdf f , i.e.,

$$\bar{\mathbf{m}}(x, t) = m_0 \int_{S^2} m f(m, t, x) \, dm.$$

In the general MPI setting we thus obtain an observation operator C_{MPI} mapping the concentration and the pdf to a time-dependent voltage measurement and a state equation M with respect to the pdf, taking the following form:

$$C_{\text{MPI}}(c, f) = -\mu_0 m_0 a * \left(\int_{\Omega} c(x) \mathbf{p}^R(x)^T \int_{S^2} m \frac{\partial}{\partial t} f(m, \cdot, x) \, dm \, dx \right) = v$$

$$(1) \quad M(f, \delta \mathbf{h}) = \frac{\partial}{\partial t} f - \operatorname{div}_{S^2} \left(\frac{1}{2\tau} \nabla_{S^2} f - \mathbf{b}(\cdot, \mathbf{H} + \delta \mathbf{h}) f \right) = 0, \quad f(\cdot, 0, \cdot) = f_0,$$

where $m_0 > 0$ is the magnetic moment of a single particle, $\mathbf{p}^R : \mathbb{R}^3 \rightarrow \mathbb{R}^3$ denotes the coil sensitivity, $a : \mathbb{R} \rightarrow \mathbb{R}$ is an analog filter function, and \mathbf{H} is the applied magnetic field as defined before. The calibration problem now takes the form of identifying a $\delta \mathbf{h}$ from given tuples (c, v) , where $\delta \mathbf{h}$ encodes unknown or uncertain aspects of the nanoparticle behavior, such as particle anisotropy or deviations in

the effective magnetic field, which may be the result of technical inaccuracies or of physical effects that have been neglected in the model formulation.

In principle, three main settings for the parameter identification problem can be distinguished. If $\delta\mathbf{h}$ is considered as a purely time-dependent function, i.e., $\delta\mathbf{h} : I \rightarrow \mathbb{R}^3$, deviations in the applied magnetic field as well as potential effective modeling of particle behavior (for example, a time-dependent effective anisotropy constant) can be covered. Taking $\delta\mathbf{h}$ as purely space-dependent, i.e., $\delta\mathbf{h} : S^2 \rightarrow \mathbb{R}^3$, a static anisotropy of arbitrary form can be described, potentially including non-anisotropy-related effects into an effective anisotropy term. The most general case, $\delta\mathbf{h} : I \times S^2 \rightarrow \mathbb{R}^3$, then allows for modeling the fully coupled case of Brownian and Néel rotation with arbitrary anisotropy. All settings might also have a dependence on the field-of-view variable $x \in \Omega$.

Numerical simulations for the first case, $\delta\mathbf{h} : I \rightarrow \mathbb{R}^3$, have been carried out and further extensions remain future work: For this setting, we consider the following adapted setup without parametric dependence on x . We note that the adaption to more general cases is straightforward in theory, but may require more careful consideration in implementation details. We consider the observation operator that takes the mean of a given probability density function, $C : W := \{f \in L^2(I, H^1(S^2)) | f' \in L^2(I, H^1(S^2)^*)\} \rightarrow L^2(I)^3$ with

$$C(f) = \int_S m f(\cdot, m) dm = \bar{\mathbf{m}},$$

and the state equation as in (1). This yields the parameter-to-state operator $\mathcal{S} : H^1(I)^3 \rightarrow W$, such that

$$M(\mathcal{S}(\delta\mathbf{h}), \delta\mathbf{h}) = 0 \quad \wedge \quad \mathcal{S}(\delta\mathbf{h})(0) = f_0,$$

and the forward operator $F : H^1(I)^3 \rightarrow L^2(I)^3$, $F = C \circ \mathcal{S}$. In this case, we have chosen $H^1(I)^3$ as a parameter space for $\delta\mathbf{h}$ to ensure some smoothness in the reconstruction; in general, a subset of an L^p -space is possible as well, ensuring well-definedness of the parameter-to-state mapping.

This setting leads to the Landweber iteration for given noisy $\bar{\mathbf{m}}^\delta$

$$\delta\mathbf{h}^{(k+1)} = \delta\mathbf{h}^{(k)} - w_k \mathcal{I} \mathcal{S}'(\delta\mathbf{h}^{(k)})^* C^*(C\mathcal{S}(\delta\mathbf{h}^{(k)}) - \bar{\mathbf{m}}^\delta),$$

where $\mathcal{I} = (\text{Id} - \Delta)^{-1}$ is the Riesz isomorphism in $H^1(I)^3$, $C^* : L^2(I)^3 \rightarrow W^*$, $(C^*v)(u) = \int_I \int_{S^2} \langle m, v(t) \rangle_{\mathbb{R}^3} u(m, t) dm dt$, and, as proven for a very general case in [1],

$$\mathcal{S}'(\delta\mathbf{h})^* z = \int_{S^2} \mathcal{S}(\delta\mathbf{h}) \left(\frac{\partial \mathbf{b}}{\partial \mathbf{h}}(m, \mathbf{H} + \delta\mathbf{h}) \right)^T \nabla_{S^2} p^z dm,$$

where $p^z \in W$ solves

$$-(p^z)'(t) = -\text{div}_{S^2} \left(\mathbf{b}(\cdot, \mathbf{H}(t) + \delta\mathbf{h}(t)) p^z(t) - \frac{1}{2\tau} \nabla_{S^2} p^z(t) \right) + z(t), \quad t \in (0, T),$$

$$p^z(T) = 0.$$

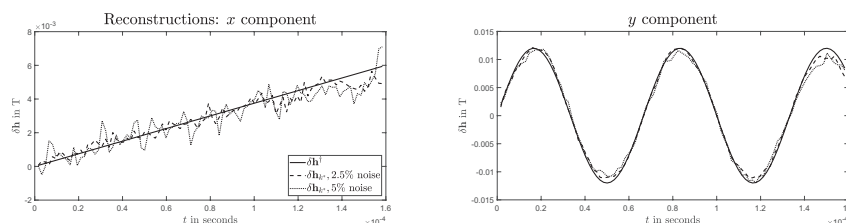


FIGURE 1. Reconstruction of x and y component of a three-dimensional applied magnetic field $\delta \mathbf{h}$ for different noise levels. The chosen domain $H^1(I)^3$ of F results in a smoothing in each iteration.

Reconstructions of the applied magnetic field for different noise levels are displayed in Fig. 1, where the iteration with the best reconstruction error is shown.

Future work includes a thorough analysis of the formulated parameter identification problem of MPI system calibration, investigation of further function space assumptions for $\delta \mathbf{h}$, and an experimental evaluation with real data.

REFERENCES

- [1] Kaltenbacher (2017). *All-at-once versus reduced iterative methods for time dependent inverse problems*. Inverse Problems, **33**(6): 064002.
- [2] Kluth (2018). *Mathematical models for magnetic particle imaging*. Inverse Problems, **34**(8): 083001.
- [3] Kluth, Szwargulski, Knopp (2019). *Towards Accurate Modeling of the Multidimensional Magnetic Particle Imaging Physics*. New J. Phys. **21**: 103032.
- [4] Knopp, Gdaniec, Möddel (2017). *Magnetic particle imaging: from proof of principle to preclinical applications*. Physics in Medicine & Biology, **62**(14), R124.

Moutard transform for the generalized analytic functions and for the conductivity equation

ROMAN NOVIKOV

(joint work with Petr Grinevich, Iskander Taimanov)

The transformations of the Darboux-Moutard type go back to the publications of T.F. Moutard [10] and G. Darboux [3]; see the survey given in [13]. Recently, we have constructed and studied Moutard type transformations for the generalized analytic functions and further for the conductivity equation. This talk is based, in particular, on the works [6]-[9] and [11], [12].

1. Generalized analytic functions

We consider the equation

$$\partial_{\bar{z}}\psi = u\bar{\psi} \text{ in } D \subseteq \mathbb{C}, \quad (1)$$

where $u = u(z)$ is a given function in D , D is open in \mathbb{C} . The functions $\psi = \psi(z)$ satisfying (1) are known as generalized analytic functions in D . The notation $f = f(z)$ does not mean that f is holomorphic. In the literature it is usually assumed that

$$u \in L_p(D), \quad p > 2, \text{ if } D \text{ is bounded.} \quad (2)$$

And it is also assumed that u has sufficient decay at infinity if D is unbounded.

The generalized analytic functions arise in PDE's and complex analysis, differential geometry, mechanics and mathematical physics. The classical theory of generalized analytic functions is presented in [1], [14.] However, before our recent works [6], [11], algebraic Moutard-type transforms going back to the article [10] were not yet considered in the framework of this theory.

2. $\bar{\partial}$ -approach to two-dimensional inverse problems

Equation (1) is one of the basic equations of the $\bar{\partial}$ -approach to two-dimensional inverse problems. In particular, the Faddeev solutions for the two-dimensional Schrödinger equation (with real-valued potential) at fixed real energy are generalized analytic functions in spectral parameter; see [4], [5]. It is well-known that this approach works very well (in all senses) when related generalized analytic functions are regular as for the case of two-dimensional electrical impedance tomography with real positive conductivity. However, it is also known that Faddeev solutions are singular generalized analytic functions if Faddeev exceptional points are present. The point is that using Moutard-type transform we reduce singular generalized analytic functions to regular ones. For more information, see [7], [9] and references therein.

3. Conductivity equation

The two-dimensional conductivity equation

$$\operatorname{div}(\sigma(x)\nabla\varphi(x)) = 0, \quad x = (x_1, x_2) \in D \subseteq \mathbb{R}^2, \quad (3)$$

reduces to (1) by formulas:

$$\psi = \sigma^{1/2}\partial_{\bar{z}}\varphi, \quad u = -\frac{1}{2}\partial_{\bar{z}}\ln\sigma, \quad (4)$$

where $\sigma \geq \sigma_0$, φ is real-valued; see [2].

Using this reduction, in [8] proceeding from results of [6] we constructed Moutard type transforms for the conductivity equation. The simplest of these transforms are given below by formulas (5)-(7).

Consider the conductivity equation

$$\operatorname{div}(\sigma(x)\nabla\psi(x)) = 0, \quad x = (x_1, x_2, \dots, x_d), \quad x \in D \subseteq \mathbb{R}^d, \quad (5)$$

in dimension $d \geq 1$ (and, in particular, in dimension $d = 3$).

Let the transform $\sigma \rightarrow \tilde{\sigma}$, $\psi \rightarrow \tilde{\psi}$ be defined by

$$\tilde{\sigma} = \mathcal{M}\sigma = f^2\sigma, \quad (6)$$

$$\tilde{\psi} = \mathcal{M}\psi = f^{-1}\psi,$$

where ψ denotes an arbitrary solution of (5), and f is a fixed solution of (5). Then the following Moutard-transformed conductivity equation holds:

$$\operatorname{div}(\tilde{\sigma}(x)\nabla\tilde{\psi}(x)) = 0, \quad x \in D \subseteq \mathbb{R}^d. \quad (7)$$

In addition, the voltage-to-current maps Λ_σ and $\Lambda_{\tilde{\sigma}}$ for equations (5) and (7) are related by the formula

$$\Lambda_{\tilde{\sigma}} = f\Lambda_\sigma f - f\sigma \frac{\partial f}{\partial \nu}. \quad (8)$$

We recall that Λ_σ is defined by

$$\Lambda_\sigma(\psi|_{\partial D}) = \nu\sigma\nabla\psi|_{\partial D} \quad (9)$$

fulfilled for all sufficiently regular solutions ψ of equation (5) in D , where D is bounded, ∂D is smooth, ν denotes the outward normal to ∂D .

In particular, formulas (5)-(9) can be used in the framework of numerical testing of algorithms of electrical impedance tomography.

Note that studies of the action of the Darboux-Moutard transforms on DtN-type boundary maps were started in [12].

REFERENCES

- [1] L. Bers, *Theory of pseudo-analytic functions*, Courant Institute of Mathematical Sciences, New York University, Institute for Mathematics and Mechanics, 1953, 187 pages.
- [2] R.M. Brown, G.A. Uhlmann, *Uniqueness in the inverse conductivity problem for nonsmooth conductivities in two dimensions*, *Commun. Partial Differ. Equ.* **22** (1997), 1009–1027.
- [3] G. Darboux, *Sur une proposition relative aux équations linéaires*, *C. R. Acad. Sci. Paris* **94** (1882), 1456–1459.
- [4] L.D. Faddeev, *Growing solutions of the Schrödinger equation*, *Sov. Phys. Dokl.* **10**(1966), 1033–1035.
- [5] P.G. Grinevich, S.P. Novikov, *Two-dimensional 'inverse scattering problem' for negative energies and generalized-analytic functions. 1. Energies below the ground state*, *Funct. Anal. Appl.* **22** (1988), 19–27.
- [6] P.G. Grinevich, R.G. Novikov, *Moutard transform for the generalized analytic functions*, *J. Geom. Anal.* **26** (2016), 2984–2995.
- [7] P.G. Grinevich, R.G. Novikov, *Moutard transform approach to generalized analytic functions with contour poles*, *Bull. Sci. Math.* **140** (2016), 638–656.
- [8] P.G. Grinevich, R.G. Novikov, *Moutard transforms for the conductivity equation*, *Lett. Math. Phys.* **109** (2019), 2209–2222.
- [9] P.G. Grinevich, R.G. Novikov, *Creation and annihilation of point-potentials using Moutard-type transform in spectral variable*, *J. Math. Phys.* **61** (2020), 093501.
- [10] T.F. Moutard, *Sur la construction des équations de la forme $\frac{1}{z} \frac{\partial^2 z}{\partial x \partial y} = \lambda(x, y)$ qui admettent une intégrale générale explicite*, *J. École Polytechnique* **45** (1878), 1–11.
- [11] R.G. Novikov, I.A. Taimanov, *Moutard type transformation for matrix generalized analytic functions and gauge transformations*, *Russian Math. Surveys* **71** (2016), 970–972.
- [12] R.G. Novikov, I.A. Taimanov, *Darboux-Moutard transformations and Poincaré-Steklov operators*, *Proc. Steklov Inst. Math.* **302** (2018), 315–324.

- [13] I.A. Taimanov, S.P. Tsarev, *On the Moutard transformation and its applications to spectral theory and soliton equations*, J. Math. Sci. **170** (2010), 371–387.
 [14] I.N. Vekua, *Generalized Analytic Functions*, Pergamon Press Ltd. 1962.

Numerical Methods for Source Power Reconstruction in Experimental Aeroacoustics

HANS-GEORG RAUMER

(joint work with Thorsten Hohage, Carsten Spehr, Daniel Ernst)

We consider the inverse source problem of reconstructing the power of a bounded, compactly supported and uncorrelated acoustic source, given the covariance operator of pressure data within a bounded measurement domain. Such problems arise for example from aeroacoustic wind tunnel experiments.

In the presented model, the sound pressure field p satisfies the convected Helmholtz equation

$$(1) \quad (k + i\mathbf{m} \cdot \nabla)^2 p + \Delta p = -Q ,$$

where k denotes the wavenumber, \mathbf{m} (s.t. $|\mathbf{m}| < 1$) the Mach vector and Q a random source. We assume that the support of Q belongs to a bounded domain $\Omega \subset \mathbb{R}^d$ (source domain), where $d \in \{2, 3\}$. Furthermore the source Q is considered to be spatially uncorrelated, therefore its covariance operator $\text{Cov}(Q)$ is given by the multiplication operator $M_q : L^2(\Omega) \rightarrow L^2(\Omega)$

$$(2) \quad (M_q v)(x) = v(x)q(x) ,$$

where the source power function q is bounded and non-negative. The observed data of this inverse problem is given by the covariance operator of the pressure field within a measurement domain $\mathbb{M} \subset \mathbb{R}^d \setminus \overline{\Omega}$. The volume potential operator between source and measurement domain is given by $G : L^2(\Omega) \rightarrow L^2(\mathbb{M})$

$$(3) \quad (Gv)(x) = \int_{\Omega} g(x, y)v(y)dy ,$$

where g denotes the Green's function of Equation 1. Using these operators, the observed covariance operator can be factorized as

$$(4) \quad GM_q G^* =: \mathcal{C}(q)$$

and $\mathcal{C}(q)$ is a Hilbert-Schmidt operator on $L^2(\mathbb{M})$. Further we have the following uniqueness result (see [1, Theorem 3.6]).

Theorem 1 (Uniqueness). *If $q_1, q_2 \in L^\infty(\Omega)$ such that $\mathcal{C}(q_1) = \mathcal{C}(q_2)$, then*

$$q_1 = q_2 .$$

We note here that the deterministic inverse source problem

$$\text{given } p \in L^2(\mathbb{M}) \text{ find } q \text{ s.t. } Gq = p$$

is not uniquely solvable since there exist so-called non radiating sources $q \in C_c^\infty(\Omega)$ such that Gq vanishes everywhere outside Ω .

The adjoint of the forward operator $\mathcal{C} : L^2(\Omega) \rightarrow \text{HS}(L^2(\mathbb{M}))$ has the following useful characterization (see [1, Proposition 4.1]).

Proposition 1 (Adjoint forward operator). *The adjoint of \mathcal{C} is given by*

$$\mathcal{C}^* : \text{HS}(L^2(\mathbb{M})) \rightarrow L^2(\Omega), \quad (\mathcal{C}^*K)(y) = \langle K, \mathcal{P}_y \rangle_{\text{HS}},$$

for $K \in \text{HS}(L^2(\mathbb{M}))$ and $y \in \Omega$ with the monopole operator $\mathcal{P}_y \in \text{HS}(L^2(\mathbb{M}))$ defined by

$$(\mathcal{P}_y\varphi)(x_1) = \int_{\mathbb{M}} g(x_1, y) \overline{g(x_2, y)} \varphi(x_2) dx_2$$

for $\varphi \in L^2(\mathbb{M})$ and $x_1 \in \mathbb{M}$.

There exist source imaging methods that estimate the source power for each point $y \in \Omega$ separately. In experimental aeroacoustics such methods are usually referred to as *Beamforming* methods. Given observed covariance data C^{obs} , the standard Beamforming imaging functional is characterized as

$$\mathcal{I}(y) = \operatorname{argmin}_{\mu \in \mathbb{C}} \|C^{\text{obs}} - \mu \mathcal{P}_y\|_{\text{HS}}^2 = \frac{\langle C^{\text{obs}}, \mathcal{P}_y \rangle_{\text{HS}}}{\|\mathcal{P}_y\|_{\text{HS}}^2} = \frac{(\mathcal{C}^*(C^{\text{obs}}))(y)}{\|\mathcal{P}_y\|_{\text{HS}}^2}.$$

The resolution of the imaging result can be improved by replacing the standard inner product $\langle \cdot, \cdot \rangle_2$ on the data space by a weighted version. For discrete and vectorized covariance data $\hat{c} \in \mathbb{C}^n$ the weighted inner product is given by

$$\langle \cdot, \cdot \rangle_W := \langle \cdot, W^{-1} \cdot \rangle_2,$$

where $W \in \mathbb{C}^{n \times n}$ is a Hermitian, positive definite matrix. Each weighting matrix then defines an imaging functional \mathcal{I}_W by replacing the standard norm in the characterizing minimization problem by the norm induced by the weighted inner product. One can show that the optimal weighting in terms of the variance is given by the covariance matrix of the correlation data $\Sigma = \text{Cov}(\hat{c})$ (see [2, Theorem 4.1]).

Theorem 2 (Minimal variance). *Let $\Sigma \in \mathbb{C}^{n \times n}$ be regular, then for any Hermitian, positive definite weighting matrix $W \in \mathbb{C}^{n \times n}$ we have*

$$\text{Var}(\mathcal{I}_\Sigma(y)) \leq \text{Var}(\mathcal{I}_W(y)).$$

Beamforming methods provide estimators for the features of the source power function rather than a quantitative reconstruction. For the latter purpose one may consider generalized Tikhonov generalization. Since the source power function appears to be sparse for many aeroacoustic applications, we consider the following Tikhonov functional with sparsity promoting mechanisms

$$(5) \quad \mathcal{J}(q) = \frac{1}{2} \|\mathcal{C}(q) - C^{\text{obs}}\|_{\text{HS}(L^2(\mathbb{M}))}^2 + \chi_A(q) + \frac{\alpha_2}{2} \|q\|_{L^2(\Omega)}^2 + \alpha_1 \|q\|_{L^1(\Omega)}.$$

Where $\alpha_1, \alpha_2 \geq 0$ and χ_A denotes the characteristic function of the set of non-negative functions $A = \{f \in L^2(\Omega) : f \geq 0 \text{ a.e.}\}$. A Tikhonov minimizer $\hat{q}_{\alpha_1, \alpha_2} \in \operatorname{argmin}\{\mathcal{J}(q)\}$ can be approximated by the *accelerated proximal gradient method* (often called *FISTA*) [3].

Acknowledgements. The author would like to thank Barbara Kaltenbacher, Herbert Egger, Roland Griesmaier and Thorsten Hohage for helpful suggestions and discussions during the workshop.

REFERENCES

- [1] T. Hohage, H.-G. Raumer and C. Spehr, *Uniqueness of an inverse source problem in experimental aeroacoustics*, *Inverse Problems* **36** (2020), 075012.
- [2] H.-G. Raumer, C. Spehr, T. Hohage and D. Ernst, *Weighted data spaces for correlation-based array imaging in experimental aeroacoustics*, *Journal of Sound and Vibration* **494** (2021), 115878.
- [3] A. Beck, *First-Order Methods in Optimization*, Society for Industrial and Applied Mathematics, 2017.

Inverse Problem for Semilinear Radiative Transport with Internal Data

KUI REN

(joint work with Ru-Yu Lai, Yimin Zhong, Ting Zhou)

Let $\Omega \subseteq \mathbb{R}^d$ ($d \geq 2$) be a domain with boundary $\partial\Omega$, and \mathbb{S}^{d-1} the unit sphere in \mathbb{R}^d . We define the phase space $X := \Omega \times \mathbb{S}^{d-1}$ and the incoming boundary of the phase space $\Gamma_- := \{(\mathbf{x}, \mathbf{v}) \mid (\mathbf{x}, \mathbf{v}) \in \partial\Omega \times \mathbb{S}^{d-1} \text{ s.t. } -\boldsymbol{\nu}(\mathbf{x}) \cdot \mathbf{v} > 0\}$, $\boldsymbol{\nu}(\mathbf{x})$ being the unit outer normal vector at $\mathbf{x} \in \partial\Omega$. We are interested in the semilinear radiative transport equation:

$$(1) \quad \begin{aligned} \mathbf{v} \cdot \nabla u + (\sigma_a + \sigma_s)u(\mathbf{x}, \mathbf{v}) + \sigma_b \langle u \rangle u(\mathbf{x}, \mathbf{v}) &= \sigma_s(\mathbf{x})Ku(\mathbf{x}, \mathbf{v}), & \text{in } X \\ u(\mathbf{x}, \mathbf{v}) &= g(\mathbf{x}, \mathbf{v}), & \text{on } \Gamma_- \end{aligned}$$

where $\langle u \rangle$ denotes the average of $u(\mathbf{x}, \mathbf{v})$ over the variable \mathbf{v} , that is,

$$(2) \quad \langle u \rangle := \int_{\mathbb{S}^{d-1}} u(\mathbf{x}, \mathbf{v}) d\mathbf{v},$$

with $d\mathbf{v}$ being the *normalized* surface measure on \mathbb{S}^{d-1} . The linear operator K is defined through the relation

$$(3) \quad Ku(\mathbf{x}, \mathbf{v}) := \int_{\mathbb{S}^{d-1}} \Theta(\mathbf{v}, \mathbf{v}')u(\mathbf{x}, \mathbf{v}') d\mathbf{v}',$$

with the kernel $\Theta(\mathbf{v}, \mathbf{v}') \geq \underline{\varrho} > 0$ being symmetric and satisfying the normalization conditions $\int_{\mathbb{S}^{d-1}} \Theta(\mathbf{v}, \mathbf{v}') d\mathbf{v}' = \int_{\mathbb{S}^{d-1}} \Theta(\mathbf{v}, \mathbf{v}') d\mathbf{v} = 1$.

Transport equations such as (1) often appear in the literature as the mathematical models to describe radiative transfer processes in heterogeneous media.

Well-posedness of the Forward Problem. Under the assumption that $\Theta(\mathbf{v}, \mathbf{v}') \geq \underline{\theta}$ for some $\underline{\theta} > 0$, and that all the coefficient functions are bounded in $L^\infty(\Omega)$:

$$(4) \quad 0 < c_0 \leq \Xi(\mathbf{x}), \sigma_a(\mathbf{x}), \sigma_s(\mathbf{x}), \sigma_b(\mathbf{x}) \leq C_0$$

for some positive constants c_0 and C_0 , we can show that the transport equation (1) is well-posed for any sufficiently small $g(\mathbf{x}, \mathbf{v}) \in L^\infty_{d\xi}(\Gamma_-)$, and solution is non-negative if the boundary source g is [8, 7].

We assume that we have data encoded in the map:

$$(5) \quad \Lambda_T : g \in L^\infty_{d\xi}(\Gamma_-) \mapsto H_T \in L^\infty(\Omega)$$

where

$$(6) \quad H_T(\mathbf{x}) = \Xi(\mathbf{x}) \left[\sigma_a(\mathbf{x}) \langle u \rangle(\mathbf{x}) + \sigma_b(\mathbf{x}) \langle u \rangle^2(\mathbf{x}) \right], \quad \mathbf{x} \in \bar{\Omega}.$$

The inverse coefficient problem we are interested in solving is the following:

(IP): Determine the triplet $(\sigma_a, \sigma_b, \sigma_s)$ in (1) from the data encoded in Λ_T defined in (5).

Inversion with Full Λ_T Data. When data encoded in the full Λ_T map are available, we can establish uniqueness and stability results on the inverse problem based on the linearization technique of Isakov and others [2, 3, 4, 5, 6] and the result of Bal-Jollivet-Jungon for the linear transport equation [1].

More precisely, let $\varepsilon > 0$ be a small parameter. We consider the following boundary value problem:

$$(7) \quad \begin{aligned} \mathbf{v} \cdot \nabla u + \sigma_a(\mathbf{x})u(\mathbf{x}, \mathbf{v}; \varepsilon) + \sigma_b \langle u \rangle u(\mathbf{x}, \mathbf{v}; \varepsilon) &= \sigma_s(\mathbf{x})K(u), & \text{in } X \\ u(\mathbf{x}, \mathbf{v}; \varepsilon) &= \varepsilon g(\mathbf{x}, \mathbf{v}), & \text{on } \Gamma_- . \end{aligned}$$

We can then show that data encoded in the operator

$$(8) \quad \Lambda_T^{(1)} : g(\mathbf{x}, \mathbf{v}) \in L^\infty_{d\xi}(\Gamma_-) \mapsto H_T^{(1)} \in L^\infty(\Omega)$$

with

$$(9) \quad H_T^{(1)}(\mathbf{x}) := \partial_\varepsilon H_T(\mathbf{x}; \varepsilon)|_{\varepsilon=0} = \Xi \sigma_a \langle u^{(1)} \rangle(\mathbf{x}), \quad u^{(1)}(\mathbf{x}, \mathbf{v}) := \partial_\varepsilon u(\mathbf{x}, \mathbf{v}; \varepsilon)|_{\varepsilon=0}$$

are sufficient to determine σ_a and σ_s , under the assumption that Ξ is known, according to a result of Bal-Jollivet-Jungon [1]. Moreover, the second order data

$$(10) \quad H_T^{(2)}(\mathbf{x}) := \partial_\varepsilon^2 H_T(\mathbf{x}, \mathbf{v})|_{\varepsilon=0} = \Xi \left(\sigma_a \langle u^{(2)} \rangle + 2\sigma_b \langle u^{(1)} \rangle \langle u^{(1)} \rangle \right)(\mathbf{x}),$$

with $u^{(2)}(\mathbf{x}, \mathbf{v}) := \partial_\varepsilon^2 u(\mathbf{x}, \mathbf{v}; \varepsilon)|_{\varepsilon=0}$ are sufficient to determine σ_b as stated in the following theorem [7].

Theorem 1. Let H_T and \tilde{H}_T be the internal data corresponding to the coefficient sets $(\Xi, \sigma_a, \sigma_b, \sigma_s)$ and $(\Xi, \sigma_a, \tilde{\sigma}_b, \sigma_s)$, both satisfying (4), respectively. Under additional mild assumptions, σ_b and $\tilde{\sigma}_b$ can be reconstructed from $H_T^{(2)}$ and $\tilde{H}_T^{(2)}$, that is,

$$(11) \quad \|\sigma_b - \tilde{\sigma}_b\|_{L^2(\Omega)} \leq C \|H_T^{(2)} - \tilde{H}_T^{(2)}\|_{L^2(\Omega)}$$

for some constant $C \geq 0$.

A similar result can be derived for the diffusion approximation to the transport equation (1); see [7] for more details.

Inversion with Finite Data Sets. In the case where we have only a finite number of data sets, the inverse problem is more complicated to analyze. In [8], we show, under some assumptions, that the coefficient pair (σ_a, σ_b) can be uniquely reconstructed from two well-selected data sets.

Corollary 1. *Let (σ_a, σ_b) and $(\tilde{\sigma}_a, \tilde{\sigma}_b)$ be two sets of absorption coefficients, and $\mathbf{H} := (H_1, H_2)$ and $\tilde{\mathbf{H}} := (\tilde{H}_1, \tilde{H}_2)$ the corresponding data generated with $\mathbf{g} = (g_1, g_2)$. Under some assumptions on the coefficients and the data, we have that, there exists constants $\mathfrak{c}, \tilde{\mathfrak{c}} > 0$ such that*

$$(12) \quad \tilde{\mathfrak{c}} \|\mathbf{H} - \tilde{\mathbf{H}}\|_{L^2(\Omega)} \leq \left\| \begin{pmatrix} \sigma_a \\ \sigma_b \end{pmatrix} - \begin{pmatrix} \tilde{\sigma}_a \\ \tilde{\sigma}_b \end{pmatrix} \right\|_{L^2(\Omega)} \leq \mathfrak{c} \|\mathbf{H} - \tilde{\mathbf{H}}\|_{L^2(\Omega)}.$$

The proof of this result is constructive. It is based on a fixed point argument that leads to an explicit reconstruction algorithm.

Parametric Sensitivity Analysis of Inversion. The derivation of the inversion results allows us to perform a sensitivity analysis on the sensitivity of the reconstruction of the absorption coefficients (σ_a, σ_b) with respect to the change of the scattering coefficient σ_s . This is something that is useful in characterizing the impact of the inaccuracy in the value of σ_s on the reconstruction of (σ_a, σ_b) .

Theorem 2. *Let (σ_a, σ_b) and $(\tilde{\sigma}_a, \tilde{\sigma}_b)$ be reconstructed with σ_s and $\tilde{\sigma}_s$ respectively, from the same data set H_T . Under additional mild assumptions, we have that,*

$$(13) \quad \|(\sigma_a - \tilde{\sigma}_a)\|_{L^2(\Omega)} + \|(\sigma_b - \tilde{\sigma}_b)\|_{L^2(\Omega)} \leq \mathfrak{c} \|(\sigma_s - \tilde{\sigma}_s)\|_{L^2(\Omega)}$$

for some constant $\mathfrak{c} > 0$.

REFERENCES

- [1] G. BAL, A. JOLLIVET, AND V. JUGNON, *Inverse transport theory of photoacoustics*, Inverse Problems, 26 (2010). 025011.
- [2] V. ISAKOV, *On uniqueness in inverse problems for semilinear parabolic equations*, Arch. Rational Mech. Anal., 124 (1993), pp. 1–12.
- [3] ———, *Uniqueness of recovery of some quasilinear partial differential equations*, Commun. PDE, 26 (2001), pp. 1947–1973.
- [4] ———, *Uniqueness of recovery of some systems of semilinear partial differential equations*, Inverse Problems, 17 (2001), pp. 607–618.
- [5] V. ISAKOV AND A. NACHMAN, *Global uniqueness for a two-dimensional elliptic inverse problem*, Trans. AMS, 347 (1995), pp. 3375–3391.
- [6] V. ISAKOV AND J. SYLVESTER, *Global uniqueness for a semilinear elliptic inverse problem*, Comm. Pure Appl. Math., 47 (1994), pp. 1403–1410.
- [7] R.-Y. LAI, K. REN, AND T. ZHOU, *Nonlinear quantitative photoacoustic imaging in transport and diffusive regimes*, Preprint, (2021).
- [8] K. REN AND Y. ZHONG, *Unique determination of absorption coefficients in a semilinear transport equation*, arXiv:2007.09516, (2020).

The influence of a fractional subdiffusion operator: A tale of two inverse problems

WILLIAM RUNDELL

(joint work with Barbara Kaltenbacher)

Fractional order calculus has a long history dating from the work of Abel two hundred years ago, but it is only relatively recently that the modelling aspects of fractional derivatives have become apparent. The standard diffusion equation is based on a random walk model of Brownian type; at each fixed time step the particles move a fixed distance in a random direction. More complex models, but again leading to parabolic equations are obtained if the fixed time steps and distances are replaced by values obtained from sampling given probability distributions provided these have sufficiently convergent moments. If this latter assumption is relaxed then one obtains a so-called anomalous diffusion process which no longer has the standard Markovian property of parabolic operators and, under specific conditions, can be shown to be equivalent to space-time differential operators of fractional order. For the case of time fractional derivatives the long-time behaviour of the solution is very different from the parabolic case: there is only linear decay for the solution as opposed to exponential decay. One consequence of this is the damping effect which with a classical time derivative gives exponential decay of all frequencies, is replaced by a more selective one where the decay is much slower. This has seen application beyond actual physical models designed specifically to take advantage of these effects. This talk were give some of the background to the above but also will illustrate the effect for two specific classes of inverse problems. The result is the severe ill-conditioning of the classical case can, again under specific circumstances, be replaced by a much milder ill-conditioning leading to much superior reconstructions.

The first inverse problem is the recovery of both the coefficients $a(x)$ and $q(x)$ in

$$\begin{aligned} D_t^\alpha u - \nabla \cdot (a \nabla u) + q u &= r_u & t \in (0, T), & & u(0) = u_0 \\ D_t^\alpha v - \nabla \cdot (a \nabla v) + q v &= r_v & t \in (0, T), & & v(0) = v_0 \end{aligned}$$

with prescribed impedance boundary and given initial conditions and subject to measured data $g_u(x) := u(x, T)$ $g_v := v(x, T)$ $x \in \Omega$. Here $0 < \alpha \leq 1$

One can prove a uniqueness result for all values of α but the inverse problem is ill-conditioned. For a given level of noise in data g and the value of T the number N of effective Fourier coefficients can be computed. In the case of the parabolic operator, $\alpha = 1$ the exponential decay of the solution with T severely limits the effective recovery of the high frequency information in both $a(x)$ and $q(x)$ resulting in poor reconstructions of all but the lowest Fourier modes; that is N is typically very small. In the fractional case the situation is similar except that N is now considerably larger resulting in superior reconstructions of these coefficients.

A second problem seeks to recover the nonlinear reaction term $f(u)$ in

$$\partial_t^\alpha u(x, t) + \mathbb{L}u(x, t) = f(u) \quad 0 < \alpha \leq 1.$$

where $\mathbb{L}u = -\nabla \cdot (a(x)\nabla u) + q(x)u$ be defined on a domain $\Omega \subset \mathbb{R}^n$ with smooth boundary $\partial\Omega$: with now *known* coefficients $a(x)$ and $q(x) \geq 0$. There is a fundamental difference between recovery of the coefficients $\{a, q\}$ and the reaction term f . In the case of $\{a, q\}$ we know their domain - Ω whereas in the case of $f(u)$ the domain is actually all values that the solution u has taken on during the evolution process. This leads to much more restrictive conditions on the allowed data. However, by projecting the differential operator onto the boundary $t = T$ a natural iteration scheme for the recovery of f is obtained.

In the case $\alpha = 1$ conditions can be given under which this scheme leads to a contraction mapping and providing both a uniqueness result and effective numerical recovery of the unknown f . For the fractional case $\alpha < 1$ the problem is much more challenging and we are only able to prove significantly weaker results.

Reconstruction formulae for diffraction tomography with optical tweezers

OTMAR SCHERZER

(joint work with Clemens Kirisits, Michael Quellmalz, Monika Ritsch-Martel, Eric Sletterqvist, Gabriele Steidl)

Introduction. We consider 3D imaging of single particles by means of optical diffraction tomography [2, 3, 4]. During the experiment the μm -sized object is trapped and moved using optical tweezers [1]. In the present mathematical studies we assume that the motion has been determined already beforehand, but can be rather irregular. This makes the derivation of reconstruction formulae as well as the numerical solution a challenging task.

Experiment. A scattering object, characterized by nonzero scattering potential f , is illuminated with a plane wave $u^{\text{inc}} = e^{ik_0 r_3}$. The scattered wave u is measured at a plane perpendicular to the direction of propagation of u^{inc} . Using optical tweezers the specimen is rotated during irradiation. The aim of diffraction tomography is to recover f from the measurements. Depending on the location of the measurement plane (relative to the object) we distinguish two experimental setups: transmission imaging and reflection imaging. A schematic overview is shown in Figure 1.

Fourier diffraction theorem. The Fourier diffraction theorem is the basis for reconstruction algorithms in diffraction tomography. Assuming that Born's approximation is valid, it relates the 2D Fourier transform of the measurements $\mathcal{F}_{1,2}u$ to the 3D Fourier transform of the scattering potential $\mathcal{F}f$:

$$\text{(FDT)} \quad \boxed{\mathcal{F}_{1,2}u(k_1, k_2, \pm r_M) = \sqrt{\frac{\pi}{2}} \frac{e^{i\kappa r_M}}{\kappa i} \mathcal{F}f(k_1, k_2, \pm\kappa - k_0).}$$

Here, $r_3 = r_M$ is the location of the measurement plane for transmission imaging, and $r_3 = -r_M$ is the location for reflection imaging. Mathematically speaking, equation (FDT) holds for all spatial frequencies $(k_1, k_2) \in \mathbb{R}^2$ such that $\kappa^2 :=$

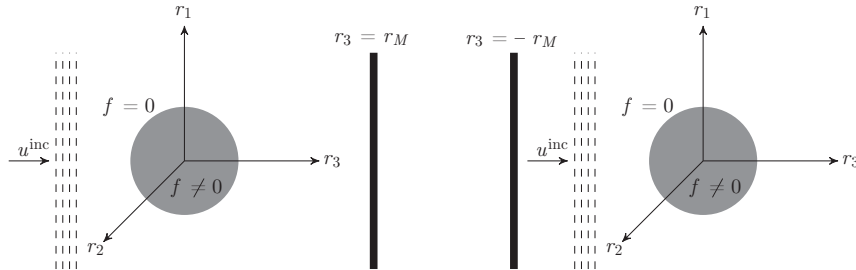


FIGURE 1. Experimental setup. The support of f is indicated by a grey ball. Left: Transmission imaging. The scattered wave is measured at the plane $r_3 = r_M$. Right: Reflection imaging. The measurement plane is located at $r_3 = -r_M$.

$k_0^2 - k_1^2 - k_2^2 \neq 0$. Practically speaking, however, only the frequencies $k_1^2 + k_2^2 < k_0^2$ are taken into account in a reconstruction process.

k-Space coverage. According to the Fourier diffraction theorem illuminating the specimen from a single direction provides access to the values of $\mathcal{F}f$ on a *semi-sphere*. However, by continuously rotating the object we can obtain knowledge of $\mathcal{F}f$ in a *volume* \mathcal{A} . In Figure 2 this volume is visualized for a full rotation about the r_1 -axis. To account for the fact that in optical trapping experiments the motion of the specimen cannot be controlled entirely, we need in general to consider rotations about a moving axis.

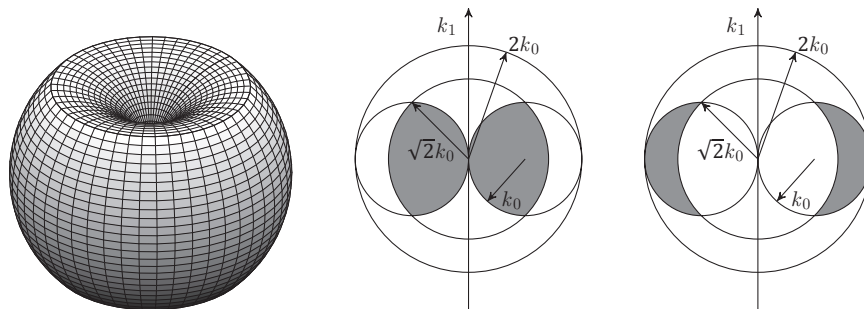


FIGURE 2. Left: Volume \mathcal{A} for transmission imaging with rotation of the specimen about the r_1 -axis. Middle: 2D slice of \mathcal{A} . Right: 2D slice of the corresponding volume for reflection imaging.

Reconstruction formula. The Fourier inversion theorem can be used to obtain an approximation of the form

$$f(\mathbf{r}) \approx (2\pi)^{-\frac{3}{2}} \int_{\mathcal{A}} \mathcal{F}f(\mathbf{k}) e^{i\mathbf{k}\cdot\mathbf{r}} d\mathbf{k}.$$

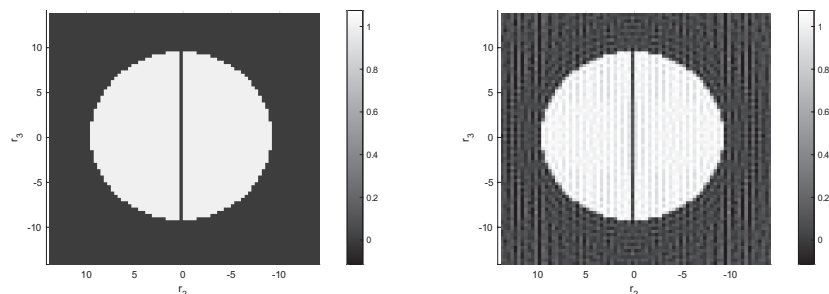


FIGURE 3. Numerical experiment for f being a characteristic function of a ball with a small segment removed. Rotation is about the r_1 -axis. Left: Slice plot of f . Right: Numerical reconstruction.

Parametrizing \mathcal{A} by means of a map T depending on k_1 , k_2 and a rotation parameter $s \in [0, 2\pi)$ we get from the Fourier diffraction theorem

$$(R) \quad f(\mathbf{r}) \approx \frac{i}{2\pi^2} \int_0^{2\pi} \int_{B_{k_0}} \kappa \mathcal{F}_{1,2} u_s(k_1, k_2, \pm r_M) e^{i(T(k_1, k_2, s) \cdot \mathbf{r} - \kappa r_M)} D d(k_1, k_2) ds,$$

where u_s denotes the scattered wave resulting from a rotation of the object according to $s \in [0, 2\pi)$, D is the Jacobian determinant of T and B_{k_0} is the disk of radius k_0 .

Numerical Tests. Figure 3 shows numerical results based on a discretization of the reconstruction formula (R).

REFERENCES

- [1] P. Jones, O. Marago, G. Volpe, *Optical Tweezers. Principles and Applications*, Cambridge University Press (2015).
- [2] A. C. Kak, M. Slaney, *Principles of Computerized Tomographic Imaging*, SIAM (2001).
- [3] F. Natterer, F. Wübbeling, *Mathematical Methods in Image Reconstruction*, SIAM (2001).
- [4] E. Wolf, *Three-dimensional structure determination of semi-transparent objects from holographic data*, Opt. Commun. **1** (1969), 153–156.

Some inverse source problems in semilinear fractional PDEs

MARIAN SLODIČKA

(joint work with Katarina Šišková)

The talk deals with some inverse source problems in time-fractional evolutionary partial differential equations. Determination of a missing source term is a hot topic in the inverse problem community in the last decades. Generally, the missing source could be a function of time and space $F(t, x)$ in transient problems. Frankly speaking, we do not have a closed theory for this class of problems. Most of the existing papers deal with separated sources $F(t, x) = h(t)f(x)$. What is an appropriate choice of an additional measurement needed for the recovery? It

depends on the situation. If $f(x)$ is missing a final time measurement is a good choice; if $h(t)$ has to be found, an (local) integral operator $\int_{\Omega} \omega(x)u(t, x) dx$ seems to sufficient for this purpose (the locality is modelled by the support of the function ω).

Can we choose a single-point time-measurement $m(t) = u(t, x_0)$ at some $x_0 \in \Omega$ to determine missing $h(t)$? It turns out that it depends on the location of x_0 . It can be shown that already in a simple example

$$(1) \quad \begin{aligned} u_t(t, x) - u_{xx}(t, x) &= h(t)f(x) & x \in \Omega = (0, 1), \\ u(0) = u(1) &= 0 \\ u(0, x) &= 0 \\ u(t, x_0) &= m(t) & x_0 \in \Omega \end{aligned}$$

we can find multiple solutions $(u(t, x), h(t))$ if x_0 is a zero point of an eigenfunction of the operator $Au = -u_{xx}$ subject to homogeneous boundary conditions. To get rid of this shortcoming one has to avoid all zero points of all eigenfunctions, which is a dense set in Ω (in our situation it is \mathbb{Q}). This is definitely a problem for computations, because of all computers work with finite decimals. To avoid this problem one can switch to non-local measurement $m(t) = \int_{\Omega} \omega(x)u(t, x) dx$ instead of a single-point measurement. Then the uniqueness of the inverse source problem can be established.

In the next part of the talk, a short introduction to fractional calculus is given. Here, the Riemann-Liouville and Caputo fractional derivatives are introduced. Both are convolution integrals with a Riemann-Liouville kernel

$$g_{\beta}(t) := \frac{t^{\beta-1}}{\Gamma(\beta)}, \quad t > 0, \beta > 0$$

which is strongly positive definite, [Nohel and Shea, 1976].

The Caputo fractional derivative can be also rewritten as

$$\partial_t^{\alpha} v(t) = \frac{\partial^{\alpha} v}{\partial t^{\alpha}} := \begin{cases} (g_{1-\alpha} * \partial_t v)(t), & \alpha \in (0, 1) \\ (g_{2-\alpha} * \partial_{tt} v)(t), & \alpha \in (1, 2) \\ \partial_t v(t), & \alpha = 1 \end{cases}$$

where $K * u$ denotes the usual convolution in time, namely

$$(K * u(x))(t) = \int_0^t K(t-s)u(x, s) ds.$$

The rest of the talk is devoted to recovery of $h(t)$ in the evolutionary time-fractional PDEs of the parabolic ($0 < \beta < 1$)

$$(g_{1-\beta} * \partial_t u(x))(t) + L(x, t)u(x, t) = h(t)f(x) + \int_0^t F(x, s, u(x, s)) ds,$$

or hyperbolic ($1 < \beta < 2$)

$$(g_{1-\beta} * \partial_{tt} u(x))(t) + L(x, t)u(x, t) = h(t)f(x) + F(x, t, u(x, t)),$$

type, where L is a general second order elliptic operator, subject to given initial and boundary conditions.

The missing $h(t)$ can be recovered from an additional measurement of the type

$$m(t) = \int_{\Omega} \omega(x)u(t, x) \, dx, \quad \text{or} \quad m(t) = \int_{\Gamma} \omega(x)u(t, x) \, d\gamma.$$

The second one represents a non-invasive measurement over a part of the boundary Γ .

Stability analysis plays a crucial role in the study of PDEs. In the process of deriving a priori estimates, the term containing the fractional derivative has to be handled in a special way. The crucial inequality for this can be found in [Slodička and Šišková, 2016], which originates from [Zacher, 2008, Zacher, 2013].

REFERENCES

- [Nohel and Shea, 1976] Nohel, J. and Shea, D. (1976). Frequency domain methods for Volterra equations. *Advances in Mathematics*, 22(3):278 – 304.
- [Slodička and Šišková, 2016] Slodička, M. and Šišková, K. (2016). An inverse source problem in a semilinear time-fractional diffusion equation. *Computers & Mathematics with Applications*, 72:1655–1669.
- [Zacher, 2008] Zacher, R. (2008). Boundedness of weak solutions to evolutionary partial integro-differential equations with discontinuous coefficients. *Journal of Mathematical Analysis and Applications*, 348(1):137 – 149.
- [Zacher, 2013] Zacher, R. (2013). A weak Harnack inequality for fractional evolution equations with discontinuous coefficients. *Annali Della Scuola Normale Superiore Di Pisa-Classe Di Scienze*, 12(4):903–940.

Beam Propagation in Random Media with Applications to Imaging and Communication

KNUT SØLNA

(joint work with Josselin Garnier)

We are interested in describing (time harmonic) wave beams propagating through a complex medium modeled as a random field. Although one may be interested in using an incoherent source beam [8] we discuss here the case with a coherent or deterministic source beam. When the beam propagates through the medium it gradually loses its coherence due to scattering. That is, the wave energy is scattered and transferred from the coherent to the incoherent part of the beam. We want to describe this process. We are not interested in describing the wave beam in a particular realization of the random medium, but rather the statistics of the wave field and how it depends on the statistics of the random medium. In fact, we describe the wave statistics via the lower order moments of the field, such moments are typically what is needed to analyze the applications we have in mind which relates to imaging and communication through a complex medium. For instance, in wireless communication when the beam propagates through a complex medium like the turbulent atmosphere, the so called fading and fluctuations of the wave intensity reaching a receiver is fundamental to describe the channel capacity or ability to communicate, see [2].

In order to reach the goal of describing the wave statistics we exploit separations of scales that are present in the problem. The main scales we consider are the central wave-length λ_0 , the beam width r_0 , the medium coherence length in range ℓ_z and in cross-range ℓ_x and also the total propagation distance L . We then consider the basic beam scaling regime:

$$\lambda_0 \ll \ell_z \sim \ell_x \sim r_0 \ll L.$$

In this scaling regime the back scattering will be very small and we arrive at a description of the forward propagating beam via the ansatz

$$\hat{u}(\omega, z, \mathbf{x}) \sim \frac{ic_0}{2\omega} e^{ikz} \hat{a}(\omega, z, \mathbf{x})$$

where \hat{u} is the solution of the (time harmonic) Helmholtz equation. Note that here we “took out” a rapidly oscillating phase with k the wave number and z the propagation or range direction, so that the wave amplitude \hat{a} oscillates relatively slower in the z direction. In the high frequency scaling limit we then arrive at a description of the wave amplitude in terms of a so called Itô-Schrödinger evolution equation derived in [3]. This is a statistical or “weak description” that can be used to deduce closed equations for all the moments of the harmonic wave field. This equation reads

$$d_z \hat{a} = \frac{1}{2ik} \Delta_{\perp} \hat{a} dz - \frac{k^2 \gamma(\mathbf{0})}{8} \hat{a} dz + \frac{ik}{2} \hat{a} dB_z$$

with B being a real valued Brownian field with covariance:

$$\mathbb{E}[B_{z_1}(\mathbf{x}_1) B_{z_2}(\mathbf{x}_2)] = \min\{z_1, z_2\} \gamma(\mathbf{x}_1 - \mathbf{x}_2)$$

where

$$\gamma(\mathbf{x}) = \int_{-\infty}^{\infty} \mathbb{E}[\mu(0, \mathbf{0}) \mu(z, \mathbf{x})] dz. \quad \gamma(\mathbf{0}) < \infty.$$

Here μ is the random field giving the random fluctuations in the medium

$$c^{-2}(z, \mathbf{x}) = c_0^{-2} \begin{cases} 1 + \mu(z, \mathbf{x}) & \text{if } z \in (0, L), \\ 1 & \text{else} \end{cases}$$

with $\mu(z, \mathbf{x})$ being centered, stationary and with coherence lengths ℓ_x, ℓ_z as mentioned above.

We now ask the question what part of the medium statistics determines the wave field statics. The first moment, or mean field $\mathbb{E}[\hat{a}(\omega, z, \mathbf{x})]$, decays exponentially fast due to scattering of the wave energy on a length scale, the so called scattering mean free path, which is determined by the one medium parameter, the medium range correlation length $\gamma(\mathbf{0})$. We remark that here we take the expectation with respect to the model for the random medium fluctuations. The second moment at range z , $\mathbb{E}[\hat{a}(\omega, z, \mathbf{x}) \bar{\hat{a}}(\omega, z, \mathbf{x} + \Delta \mathbf{x})]$, can also be derived explicitly. However, this cross moment depends in general on the full spectrum $\gamma(\mathbf{x})$. In order to describe in particular the fluctuations of the intensity of the transmitted wave field one needs the fourth moment of the wave field. The Itô-Schrödinger equation leads to a transport equation for the fourth moment, but an explicit solution for this is not known. In [5] we show however that an explicit description for the fourth

moment can be obtained in a secondary scaling regime, the so called scintillation regime, corresponding to a relatively broad beam or r_0 larger than ℓ_x . In fact, the resulting description corresponds to a quasi Gaussian property in that the fourth moment can be described in terms of the second moment as in the case of a Gaussian random field. The wave description we just outlined is used in particular in [6] to analyze a so called speckle imaging configuration. Here the statistics of the transmitted speckle, a fourth order quantity, is used in a source imaging procedure.

We summarize the complexity of the wave descriptions outlined above. We start out with the Helmholtz equations for the random field in a random medium which is typically prohibitive to solve numerically in the applications we have in mind due to the relatively short wave length and rapid medium fluctuations. Then we identify in the high frequency scaling regime the Itô-Schrödinger equation which may form the basis for feasible numerically simulations via so called phase screen methods. Moreover, this description leads to explicit descriptions for the first two wave moments. The fourth moment derives from a complicated transport equation, a pde with in general eight lateral coordinates in addition to the range coordinate. However, in the so called scintillation regime we arrive at explicit expressions also for the fourth moment, a description that is important in a number of applications.

We next remark on a medium fabric imaging configuration. We assume here an anisotropic medium scaling so that

$$\lambda_0 \sim \ell_z \ll \ell_x \sim r_0 \ll L.$$

In this case the backscattering from the medium will be stronger than in the scale isotropic case described above. In this case the medium parameters that determine the backscattered wave spectrum are in the simplest case

$$\Delta_{\mathbf{x}}\tilde{\gamma}(0, \mathbf{0}), \quad \tilde{\gamma}(2k, \mathbf{0}), \quad \Delta_{\mathbf{x}}\tilde{\gamma}(2k, \mathbf{0}),$$

for

$$\tilde{\gamma}(k, \boldsymbol{\kappa}) = \int \int \mathbb{E}[\mu(0, \mathbf{0})\mu(z, \mathbf{x})]e^{i(zk + \mathbf{x} \cdot \boldsymbol{\kappa})} dz d\mathbf{x}.$$

Here the argument $2k$ reflects the coupling between the forward propagating and reflected waves. In general the medium may be only “locally stationary” so that the above parameters vary with respect to range and in [4] we describe how measurement of in particular the (spectral) dynamic width of the backscattered wave energy can be used in an imaging procedure for the changes in the medium statistics with respect to range.

We finally remark that above we discussed relatively long range propagation. It is also of interest to describe the wave corruption over relatively short ranges, for instance for so called “last mile” links in communication applications. In this case different tools need to be used for the wave description and work on such a characterization is in progress [7].

REFERENCES

- [1] L.C. Andrews and R.L. Phillips, *Laser Beam Propagation through Random Media*, SPIE, Bellingham, 2005.
- [2] L. Borcea, J. Garnier and K. Sølna, *Multiplexing schemes for optical communication through atmospheric turbulence*, J. Opt. Soc. Am. A **37**(5) (2020), 720–730.
- [3] J. Garnier and K. Sølna, *Coupled paraxial wave equations in random media in the white-noise regime*, Ann. Appl. Probab., **19** (2009), 318–346.
- [4] J. Garnier and K. Sølna, *Background Velocity Estimation by Cross Correlation of Ambient Noise Signals in the Radiative Transport Regime*, Comm. Math. Sci., **9**(3) (2011), 743–766.
- [5] J. Garnier and K. Sølna, *Fourth-moment analysis for beam propagation in the white-noise paraxial regime*, Arch. Rational Mech. Anal. **220** (2016), 37–81.
- [6] J. Garnier and K. Sølna, *Imaging through a scattering medium by speckle intensity correlations*, Inverse Problems, **34**:9 (2018), 094003.
- [7] J. Garnier and K. Sølna, *Short- and Long-Range Paraxial Propagation*, Preprint (2020).
- [8] G. Gbur, *Partially coherent beam propagation in atmospheric turbulence*, J. Opt. Soc. Am. A, **31** (2014), 2038–2045.
- [9] J.W. Strohbehn, *Laser beam propagation in the atmosphere*. Springer, Berlin (1978)

The Noise Collector for sparse recovery in high dimensions

CHRYSOULA TSOGKA

(joint work with Miguel Moscoso, Alexei Novikov and George Papanicolaou)

We are interested in imaging sparse scenes, accurately, using limited and noisy data. Such imaging problems arise in many areas such as medical imaging, structural biology, radar and geophysics. Both the passive and the active array imaging problems with or without multiple scattering can be reduced to finding the solution of a linear system of the form

$$\mathcal{A}\boldsymbol{\rho} = \mathbf{b}_0 + \mathbf{e},$$

where \mathbf{e} is the noise. It is well known, that a sparse solution of this system can be found efficiently with an ℓ_1 -norm minimization approach,

$$(1) \quad \boldsymbol{\rho}_* = \arg \min_{\boldsymbol{\rho}} \|\boldsymbol{\rho}\|_{\ell_1}, \text{ subject to } \mathcal{A}\boldsymbol{\rho} = \mathbf{b}_0 + \mathbf{e},$$

if the data is noiseless. However, determining $\boldsymbol{\rho}$ from data corrupted by noise is still a challenging problem. For optimal results, current approaches need to tune parameters that depend on the level of noise, which is often difficult to be estimated in practice. In this talk, the Noise Collector [1, 2], a new parameter-free, ℓ_1 norm minimization approach was presented. In lieu of (1), we solve the augmented system

$$(2) \quad (\boldsymbol{\rho}_\tau, \boldsymbol{\eta}_\tau) = \arg \min_{\boldsymbol{\rho}, \boldsymbol{\eta}} (\tau \|\boldsymbol{\rho}\|_{\ell_1} + \|\boldsymbol{\eta}\|_{\ell_1}), \\ \text{subject to } \mathcal{A}\boldsymbol{\rho} + \mathcal{C}\boldsymbol{\eta} = \mathbf{b}_0 + \mathbf{e},$$

where τ is an $O(1)$ *no-phantom* weight and \mathcal{C} is the Noise Collector matrix. The unknown $\boldsymbol{\eta}$ does not correspond to a physical quantity. It is introduced to provide an appropriate linear combination of the columns of \mathcal{C} that produces a good approximation to the noise vector \mathbf{e} .

The Noise Collector has a zero false discovery rate (no false positives) for any level of noise, with probability that tends to one as the dimension of \mathbf{b}_0 increases to infinity and provides exact support recovery when the noise is not too large. A Fast Noise Collector Algorithm has been implemented which makes the computational cost of solving the minimization problem comparable to the original one. The effectiveness of the method has been demonstrated in imaging applications.

REFERENCES

- [1] M. Moscoso, A. Novikov, G. Papanicolaou and C.Tsogka, Imaging with highly incomplete and corrupted data, *Inverse Problems*, 36(3), p. 035010, 2020.
- [2] M. Moscoso, A. Novikov, G. Papanicolaou and C.Tsogka, The Noise Collector for sparse recovery in high dimensions, *Proceedings of the National Academy of Sciences*, 117 (21), p. 11226-11232, 2020.

Proximal gradient methods applied to optimization problems with L^p -cost, $p \in [0, 1)$

DANIEL WACHSMUTH

(joint work with Carolin Natemeyer)

Let $\Omega \subset \mathbb{R}^n$ be Lebesgue measurable with finite measure. We consider a possibly non-smooth optimal control problem of type

$$(P) \quad \min_{u \in L^2(\Omega)} f(u) + \int_{\Omega} g(u(x)) dx.$$

Here, the function $g : \mathbb{R} \rightarrow \mathbb{R} \cup \{+\infty\}$ is nonconvex and nonsmooth. In this report, we restrict ourselves to

$$g(u) = |u|^p, \quad p \in (0, 1),$$

and

$$g(u) = |u|_0 := \begin{cases} 1 & \text{if } u \neq 0 \\ 0 & \text{if } u = 0. \end{cases}$$

The function $f : L^2(\Omega) \rightarrow \mathbb{R}$ is assumed to be continuously Frechet differentiable. Here, we have in mind to choose $f(u) := f(y(u))$ as the smooth part of an optimal control problem incorporating the state equation and possibly smooth cost functional.

Due to the lack of weak sequentially lower semicontinuity of $u \mapsto \int_{\Omega} g(u(x)) dx$ one cannot prove existence of solutions. In fact, one can construct problems that have no solutions, [1]. In the case that a solution exists, we can characterize it by the Pontryagin maximum principle.

Let us describe and analyze the proximal gradient algorithm. For details and proofs, we refer to the technical report [2].

Algorithm 1. Choose $L > 0$ and $u_0 \in L^2(\Omega)$. Set $k = 0$.

(1) Compute u_{k+1} as solution of

$$(1) \quad \min_{u \in L^2(\Omega)} f(u_k) + \nabla f(u_k)(u - u_k) + \frac{L}{2} \|u - u_k\|_{L^2(\Omega)}^2 + g(u).$$

(2) Set $k := k + 1$, repeat.

The minimization problem (1) can be solved by means of pointwise a.e. minimization. In the case $p = 0$, there is an explicit formula for the solution [1]. For $p \in (0, 1)$, one has to carry out some iterative optimization method to compute a global minimum.

We have the following result regarding convergence. We assume that ∇f is Lipschitz continuous with modulus L_f . Let χ_k denote the characteristic function of the support of (u_k) .

Theorem 2. For $L > L_f$ let (u_k) be a sequence of iterates generated by Algorithm 1. Then the following statements hold:

- (1) The sequence $(f(u_k) + j(u_k))$ is monotonically decreasing and converging.
- (2) The sequences (u_k) and $(\nabla f(u_k))$ are bounded in $L^2(\Omega)$ if $f + j$ is weakly coercive on $L^2(\Omega)$, i.e., $f(u) + j(u) \rightarrow \infty$ as $\|u_k\|_{L^2(\Omega)} \rightarrow \infty$.
- (3) $\|u_{k+1} - u_k\|_{L^2(\Omega)} \rightarrow 0$.
- (4) The sequence of characteristic functions (χ_k) is converging in $L^1(\Omega)$ and pointwise a.e. to some characteristic function χ .

The condition $L > L_f$ is important to prove (1)–(3). In order to prove (4), we employ the following property of solutions of (1): There exists $u_0 > 0$ such that for almost all $x \in \Omega$

$$u_{k+1}(x) = 0 \text{ or } |u_{k+1}(x)| \geq u_0.$$

Additional results in the case $p = 0$ can be found in [1]. Unfortunately it is not possible to prove that a weak limit point u^* of the iterates satisfy the Pontryagin maximum principle. Due to the presence of the additional quadratic term with factor $L > 0$, we can at best hope to prove that in the limit we have

$$u^*(x) = \arg \min_{u \in \mathbb{R}} \nabla f(u^*)(x) \cdot u + \frac{L}{2} (u^*(x) - u)^2 + g(u).$$

Here, the set of all points $(\nabla f(u^*)(x), u^*(x))$ satisfying this relation is non-convex. Hence, passing to the weak limit will introduce some additional convexification. For details, we refer to [2].

REFERENCES

- [1] D. Wachsmuth. Iterative hard-thresholding applied to optimal control problems with $L^0(\Omega)$ control cost. *SIAM J. Control Optim.*, 57(2):854–879, 2019.
- [2] C. Natemeyer, D. Wachsmuth. A proximal gradient method for control problems with non-smooth and nonconvex control cost. <http://arxiv.org/abs/2007.11426>, 2020.

Parameter identification for the Landau-Lifshitz-Gilbert equation in Magnetic Particle Imaging

ANNE WALD

(joint work with Tram T. N. Nguyen, Barbara Kaltenbacher, Thomas Schuster)

Magnetic particle imaging (MPI) is a relatively new imaging technique aiming at the reconstruction of magnetic nano-particles (serving as tracers) to visualize, e.g., the blood flow in the cardiovascular system (see also [6, 7]). The signal generation is based on the response of the magnetic nano particles to a dynamic external magnetic field with a field-free point (FFP): The FFP is driven through the field-of-view and the magnetization of the magnetic particles undergoes an abrupt change when the FFP passes them (which assures the inclusion of local information on the particle concentration in the signal generation). This change in the magnetization generates a time-dependent voltage in the receive coils, which serves as data.

The forward problem of MPI is formulated by

$$v_l(t) = \int_0^T \tilde{a}_l(t - \tau) \int_{\Omega} c(\mathbf{x}) s_l(\mathbf{x}, \tau) \, d\mathbf{x} \, d\tau,$$

where c is the space-dependent particle concentration, v_l the voltage measured in the l -th ($l = 1, \dots, L$) receive coil, s the system function, and the function \tilde{a} serves as a filter that separates the particle signal from the external field. The system function encodes the underlying physical model, i.e., the interaction of the external field and the particle magnetization.

There are two different inverse problems arising in MPI: The actual imaging problem, where the concentration is to be determined from the measured particle signals using a pre-computed system function, and the calibration problem, which refers to the calculation of the system function from data that is generated in calibration scans, i.e., scans for known particle concentrations.

We address the calibration problem: The system function is modeled as

$$s_l(\mathbf{x}, t) = \mathbf{p}_l^R \cdot \partial_t \mathbf{m}(\mathbf{x}, t)$$

with the coil sensitivity \mathbf{p}_l^R and the particle magnetization $\mathbf{m}(\mathbf{x}, t)$. In our approach, the concentration is a dimensionless quantity that can be interpreted as a characteristic function.

Inspired by models from micromagnetism ([2]), we use the Landau-Lifshitz-Gilbert (LLG) equation

$$\frac{\partial}{\partial t} \mathbf{m} = -\tilde{\alpha}_1 \mathbf{m} \times (\mathbf{m} \times \mathbf{H}_{\text{eff}}) + \tilde{\alpha}_2 \mathbf{m} \times \mathbf{H}_{\text{eff}}$$

to model the evolution of the particle magnetization in response to an external applied magnetic field. The effective field \mathbf{H}_{eff} encodes various physical effects: in particular, it contains the external field \mathbf{H}_{ext} and can be extended to include, for example, the exchange within the magnetic material itself, such that

$$\mathbf{H}_{\text{eff}} = 2A\Delta\mathbf{m} + \mu_0 m_S \mathbf{H}_{\text{ext}}$$

with the exchange stiffness constant A , the magnetic permeability μ_0 and the saturation magnetization m_S .

The calibration problem in MPI is thus formulated as an inverse problem as follows: For a given set of known concentrations $c_k(\mathbf{x})$, $k = 1, \dots, K$ (e.g., delta samples $c_k(\mathbf{x}) = \chi_{V_k}(\mathbf{x})$ with a voxel V_k), we measure the corresponding induced currents

$$v_{kl}(t) = \int_0^T \tilde{a}_l(t - \tau) \int_{\Omega} c_k(\mathbf{x}) \mathbf{p}_l^R(\mathbf{x})^T \partial_t \mathbf{m}(\tau, \mathbf{x}) \, d\mathbf{x} \, d\tau.$$

The goal is to determine the system function $s_l(\mathbf{x}, t) = \mathbf{p}_l^R(\mathbf{x})^T \partial_t \mathbf{m}(t, \mathbf{x})$, $l = 1, \dots, L$, from the knowledge of $v_{kl}(t)$, $t \in [0, T]$, under the constraint that \mathbf{m} solves the LLG equation.

We use an equivalent formulation of the LLG equation:

$$\begin{aligned} \hat{\alpha}_1 m_S^2 \mathbf{m}_t - \hat{\alpha}_2 \mathbf{m} \times \mathbf{m}_t - m_S^2 \Delta \mathbf{m} &= |\nabla \mathbf{m}|^2 \mathbf{m} \\ &\quad + m_S^2 \mathbf{h}_{\text{ext}} - \langle \mathbf{m}, \mathbf{h}_{\text{ext}} \rangle \mathbf{m} \quad \text{in } [0, T] \times \Omega \\ 0 &= \partial_\nu \mathbf{m} \quad \text{on } [0, T] \times \partial\Omega \\ \mathbf{m}_0 &= \mathbf{m}(t = 0), \quad |\mathbf{m}_0| = m_S \quad \text{in } \Omega. \end{aligned}$$

In particular, the constants $\hat{\alpha}_1, \hat{\alpha}_2$ are unknown and need to be determined.

We define the forward operator by

$$F : \mathcal{W} \rightarrow \mathcal{V},$$

where

$$F(\hat{\alpha}_1, \hat{\alpha}_2, \mathbf{m})_{kl} = \int_0^T \tilde{a}_k(t - \tau) \int_{\Omega} c_l(\mathbf{x}) \mathbf{p}_k^R(\mathbf{x})^T \partial_t \mathbf{m}(\tau, \mathbf{x}) \, d\mathbf{x} \, d\tau$$

and \mathbf{m} solves the initial boundary value problem based on the LLG equation.

Since the LLG equation has a unique solution, we can formulate the inverse problem in the classical reduced formulation

$$F(\hat{\alpha}) = y,$$

where $y := (v_{k,l})_{k,l}$ and

$$F : \mathcal{D}(F) (\subseteq \mathcal{X}) \rightarrow \mathcal{Y}, \quad \hat{\alpha} = (\hat{\alpha}_1, \hat{\alpha}_2) \mapsto \mathcal{K} \frac{\partial}{\partial t} S(\hat{\alpha})$$

containing the parameter-to-state map

$$S : \mathcal{X} \rightarrow \tilde{\mathcal{U}}$$

that maps the parameters $\hat{\alpha}$ to the solution $\mathbf{m} := S(\hat{\alpha})$ of the LLG initial boundary value problem and the observation operator \mathcal{K} . Here, we have $\mathcal{X} = \mathbb{R}^2$ (parameter space) and $\mathcal{Y} = L^2([0, T])^{KL}$ (image space).

In addition, we consider the inverse problem in the all-at-once formulation (see also [1]):

$$\mathbb{F}(\mathbf{m}, \alpha_1, \alpha_2) = \begin{pmatrix} \text{(LLG)} \\ \partial_\nu \mathbf{m} \\ \mathbf{m}(t=0) - \mathbf{m}_0 \\ F(\mathbf{m})[c_k] \end{pmatrix} = \begin{pmatrix} 0 \\ 0 \\ 0 \\ (v_{kl})_{kl} \end{pmatrix} =: \mathbb{Y},$$

where

$$\text{(LLG)} := \hat{\alpha}_1 m_S^2 \mathbf{m}_t - \hat{\alpha}_2 \mathbf{m} \times \mathbf{m}_t - m_S^2 \Delta \mathbf{m} - |\nabla \mathbf{m}|^2 \mathbf{m} - m_S^2 \mathbf{h}_{\text{ext}} + \langle \mathbf{m}, \mathbf{h}_{\text{ext}} \rangle \mathbf{m}.$$

The mathematical analysis (see [3]) of the inverse problem in the two formulations yields

- The forward operator $\mathbb{F} : \mathcal{U} \times \mathbb{R}^2 \rightarrow \mathcal{W} \times L^2([0, T])^{KL}$ from the all-at-once setting is well-defined for

$$\mathcal{U} = \{ \mathbf{u} \in L^2(0, T; H_N^2(\Omega; \mathbb{R}^3)) \cap H^1(0, T; L^2(\Omega; \mathbb{R}^3)) : \mathbf{u}(0) = 0 \}$$

$$\mathcal{W} = H^1(0, T; H^1(\Omega; \mathbb{R}^3))^*$$

with $\mathbf{h}_{\text{ext}} \in L^2(0, T; L^2(\Omega; \mathbb{R}^3))$.

- If we set the state space to be $\mathcal{U} := H^1(0, T; L^2(\Omega; \mathbb{R}^3))$, the forward operator

$$F : \mathbb{R}^2 \rightarrow L^2([0, T])^{KL}$$

is well-defined.

- Both the forward operator \mathbb{F} from the all-at-once formulation and the forward operator F from the reduced formulation are Fréchet differentiable.

The inverse problem can thus be solved by the Landweber iteration in both formulations (see also [5]). In particular, the Landweber iteration for the all-at-once formulation can be seen as a solver for the LLG equation, see [4].

REFERENCES

- [1] B. Kaltenbacher, *All-at-once vs. reduced iterative methods for time-dependent inverse problems*, Inverse Problems 33 (2017) 064002.
- [2] M. Kruzik and A. Prohl, *Recent developments in the modeling, analysis, and numerics of ferromagnetism*. In SIAM review 48.3 (2006), 439–483.
- [3] B. Kaltenbacher, T. T. N. Nguyen, A. Wald, T. Schuster, *Parameter identification for the Landau-Lifshitz-Gilbert equation in Magnetic Particle Imaging*, Time-dependent Problems in Imaging and Parameter Identification, B. Kaltenbacher, T. Schuster, A. Wald (Eds.), Springer 2021
- [4] T. T. N. Nguyen, A. Wald, *On numerical aspects of parameter identification for the Landau-Lifshitz-Gilbert equation*, submitted in January 2021
- [5] T. T. N. Nguyen, *Landweber–Kaczmarz for parameter identification in time-dependent inverse problems: all-at-once versus reduced version*, Inverse Problems 35 (2019), 035009
- [6] T. Knopp, T. Buzug, *Magnetic Particle Imaging: An Introduction to Imaging Principles and Scanner Instrumentation*, Springer, Berlin/Heidelberg, 2012
- [7] B. Gleich, J. Weizenecker, *Tomographic imaging using the nonlinear response of magnetic particles*, Nature, 435 (2005), 1214–1217.

A reduced order model approach to inverse scattering in lossy layered media

JÖRN ZIMMERLING

(joint work with Liliana Borcea, Vladimir Druskin)

We introduce a reduced order model (ROM) methodology for inverse electromagnetic wave scattering in layered lossy media, using data gathered by an antenna which generates a probing wave and measures the time resolved reflected wave. We recast the wave propagation problem as a passive infinite-dimensional dynamical system, whose transfer function is expressed in terms of the measurements at the antenna. The ROM is a low-dimensional dynamical system that approximates this transfer function. While there are many possible ROM realizations, we are interested in one that preserves passivity and in addition is: (1) data driven (i.e., is constructed only from the measurements) and (2) it consists of a matrix with special sparse algebraic structure, whose entries contain spatially localized information about the unknown dielectric permittivity and electrical conductivity of the layered medium. Localized means in the intervals of a special finite difference grid.

Using some mathematical transformations, it is possible to derive from Maxwell's equations in the temporal Laplace domain, under the assumption of linear polarization of the waves, with u modeling the component of the electric field and \hat{u} the component of the magnetic field, the following system of ODE's

$$(1) \quad [\mathcal{L} + \mathcal{R}(T) + s\mathcal{Z}(T)] \begin{pmatrix} u(T, s) \\ \hat{u}(T, x) \end{pmatrix} = \begin{pmatrix} \delta(T - 0+) \\ 0 \end{pmatrix}, \quad T \in (0, T_L),$$

with boundary conditions

$$(2) \quad u(T_L, s) = 0 \quad \hat{u}(0, s) = 0$$

Here T is the travel time, related to the coordinate along which the medium varies by a bijective mapping using the wave speed. The differential operator

$$(3) \quad \mathcal{L} = \begin{pmatrix} 0 & \partial_T \\ \partial_T & 0 \end{pmatrix}$$

is skew-symmetric and

$$(4) \quad \mathcal{R}(T) = \begin{pmatrix} r(T)\zeta(T)^{-1} & 0 \\ 0 & 0 \end{pmatrix} \text{ and } \mathcal{Z}(T) = \begin{pmatrix} \zeta(T)^{-1} & 0 \\ 0 & \zeta(T) \end{pmatrix}$$

are multiplication operators. The loss coefficient r is defined as the ratio of the electrical conductivity σ and the dielectric permittivity ε , and ζ is the wave impedance, determined by ε and the magnetic permeability μ , which is usually a constant.

The system (1) is known as port-Hamiltonian [2, 1] and there is a lot of effort in the reduced-order modeling community to construct ROMs that approximate its transfer function

$$(5) \quad D(s) = \int_0^{T_L} (\delta(T) \ 0) [\mathcal{L} + \mathcal{R}(T) + s\mathcal{Z}(T)]^{-1} \begin{pmatrix} \delta(T - 0+) \\ 0 \end{pmatrix} dT,$$

which (in this particular setting) can be shown to be a meromorphic function [6] with a set of poles and zeros closed under conjugation.

To formulate the inverse problem, we use the poles and residues representation of the transfer function $D(s)$, and assume that the poles are simple. The data driven ROM we construct has the transfer function

$$(6) \quad D_n^{\text{ROM}}(s) = \sum_{j=1}^n \left[\frac{y_j}{s - \lambda_j} + \frac{\bar{y}_j}{s - \bar{\lambda}_j} \right],$$

which shares the first n poles $(\lambda_j)_{j=1}^n$ and residues $(y_j)_{j=1}^n$ with $D(s)$. The inverse problem we solve can thus be formulated as: *Given the first n poles $(\lambda_j)_{j=1}^n$ and residues $(y_j)_{j=1}^n$ of $D(s)$ compute estimates of the impedance $\zeta(T)$ and the loss $r(T)$.*

Using the poles and residues one can construct a unique tridiagonal, linear algebraic system that matches this transfer-function and is of the form

$$(7) \quad D_n^{\text{ROM}}(s) = \mathbf{e}_1^T [\mathcal{L} + \mathcal{R} + s\mathcal{Z}]^{-1} \mathbf{e}_1 (\hat{h}_1)^{-1}$$

by solving the associated inverse eigenvalue problem with the J-symmetric Lanczos algorithm [7]. This algorithm defines the real $2n \times 2n$ ROM matrices \mathcal{L} , \mathcal{R} and \mathcal{Z} . To be more specific, the bidiagonal matrix

$$\mathcal{L} = \text{diag}[(\hat{h}_1^{-1}, h_1^{-1}, \dots, \hat{h}_n^{-1}), 1] - \text{diag}[(h_1^{-1}, \hat{h}_2^{-1}, \dots, h_n^{-1}), -1],$$

where $\text{diag}[(\dots), 1]$ denotes the superdiagonal and $\text{diag}[(\dots), -1]$ the subdiagonal, can be interpreted as a discrete analogue of the operator \mathcal{L} . Further, the grid steps h_j/\hat{h}_j are only weakly dependent on the medium and can therefore be computed independently of the medium as shown in [4]. The diagonal matrices

$$\mathcal{R} = \text{diag}(\mathbf{r}_1/\zeta_1, \hat{\mathbf{r}}_1\hat{\zeta}_1, \dots, \mathbf{r}_n/\zeta_n, \hat{\mathbf{r}}_n\hat{\zeta}_n), \quad \mathcal{Z} = \text{diag}(1/\zeta_1, \hat{\zeta}_1, \dots, 1/\zeta_n, \hat{\zeta}_n),$$

look like discretizations of the multiplication operators $\mathcal{R}(T)$ and $\mathcal{Z}(T)$. However, the analogy is not right because in \mathcal{R} there are artificial dual losses $(\hat{\mathbf{r}}_j)_{j=1}^n$ that may have negative values. The main difficulty in using the ROM for this inverse problem is interpreting these nonphysical dual losses. We recently obtained the following two reconstruction results for media with constant loss and for media with a small variation in loss.

Defining the primary grids points

$$(8) \quad T_j = \sum_{p=1}^{j-1} h_p, \quad j = 2, \dots, n+1, \quad T_1 = 0,$$

that are interlaced with the dual points

$$(9) \quad \hat{T}_j = \sum_{p=1}^j \hat{h}_p, \quad j = 1, \dots, n, \quad \hat{T}_0 = 0.$$

we obtain the following result for media with constant losses.

Proposition 1. Consider the data driven ROM computed from the first n poles and residues. Extract the coefficients $(\zeta_j, \hat{\zeta}_j)_{j=1}^n$ from the ROM using the grid steps $(h_j, \hat{h}_j)_{j=1}^n$. Let $\zeta^{(n)}(T)$ be some interpolation (e.g., piecewise constant or linear) of these coefficients on the grid (8)–(9) i.e.,

$$(10) \quad \zeta^{(n)}(T_j) = \zeta_j, \quad \zeta^{(n)}(\hat{T}_j) = \hat{\zeta}_j, \quad j = 1, \dots, n.$$

Then, $\zeta^{(n)}(T) \rightarrow \zeta(T)$ pointwise and in $L^1([0, T_L])$ as $n \rightarrow \infty$.

Further one can show that the ROM loss coefficients satisfy $\mathfrak{r}_j = r_0$ and $\hat{\mathfrak{t}}_j = 0$, for $j = 1, \dots, n$ and a direct interpretation of the ROM coefficients is possible. For media with small variations in loss we find the following.

Proposition 2. Suppose that the loss function satisfies

$$(11) \quad r(T) = r_0 + \alpha\rho(T), \quad \sup_{T \in (0, T_L)} |\rho(T)|/r_0 = O(1), \quad 0 < \alpha \ll 1.$$

Then, we have the following pointwise ROM based estimate of the impedance

$$(12) \quad \zeta^{(n)}(T) = \zeta(T)[1 + o(1) + O(\alpha^2)].$$

Moreover, the functions $\mathfrak{r}^{(n)}(T)$ and $\hat{\mathfrak{t}}^{(n)}(T)$ are of the form

$$(13) \quad \mathfrak{r}^{(n)}(T) = r_0 + \alpha\rho^{(n)}(T)[1 + o(1) + O(\alpha)], \quad \hat{\mathfrak{t}}^{(n)}(T) = \alpha\hat{\rho}^{(n)}(T)[1 + o(1) + O(\alpha)],$$

where the $O(\alpha)$ terms satisfy

$$(14) \quad \int_0^{T_L} \rho(T) \frac{\phi_j^2(T)}{\zeta_j(T)} dT = \int_0^{T_L} \left[\rho^{(n)}(T) \frac{\phi_j^2(T)}{\zeta_j(T)} + \hat{\rho}^{(n)}(T) \zeta(T) \hat{\phi}_j^2(T) \right] dT,$$

$$(15) \quad \int_0^{T_L} \rho(T) \frac{\psi_j^2(T)}{\zeta_j(T)} dT = \int_0^{T_L} \left[\rho^{(n)}(T) \frac{\psi_j^2(T)}{\zeta_j(T)} + \hat{\rho}^{(n)}(T) \zeta(T) \hat{\psi}_j^2(T) \right] dT,$$

for $j \geq 1$. Here $o(1)$ is in the limit $n \rightarrow \infty$ and $\phi, \psi, \hat{\phi}$ and $\hat{\psi}$ are (computatable) eigenfunctions associated with certain Sturm-Liouville problems.

More details can be found in [5]. In the future we will try to extend this framework to higher spatial dimensions with the help of block-linear algebraic formulations as done for the lossless case in [3] and to the case of strongly varying losses.

REFERENCES

[1] S. GUGERCIN, R. POLYUGA, C. BEATTIE, AND A. VAN DER SCHAFT, *Structure-preserving tangential interpolation for model reduction of port-hamiltonian systems*, Automatica, 48 (2012), pp. 1963–1974.
 [2] P. BENNER, P. GOYAL, AND P. VAN DOOREN, *Identification of port-Hamiltonian systems from frequency response data*, Systems & Control Letters, 143 (2020), p. 104741.
 [3] L. BORCEA, V. DRUSKIN, A. MAMONOV, M. ZASLAVSKY, AND J. ZIMMERLING, *Reduced order model approach to inverse scattering*, SIAM Imaging Sciences, 13 (2019), pp. 685–723.
 [4] L. BORCEA, V. DRUSKIN, AND L. KNIZHNERMAN, *On the continuum limit of a discrete inverse spectral problem on optimal finite difference grids*, Communications on Pure and Applied Mathematics: A Journal Issued by the Courant Institute of Mathematical Sciences, 58 (2005), pp. 1231–1279.

- [5] L. BORCEA, V. DRUSKIN, AND J. ZIMMERLING, *A reduced order model approach to inverse scattering in lossy layered media*, arxiv:2012.00861, (2020), *preprint*
- [6] N. PRONSKA, *Spectral properties of sturm-liouville equations with singular energy-dependent potentials*, arXiv preprint arXiv:1212.6671, (2012).
- [7] Y. SAAD, *The Lanczos biorthogonalization algorithm and other oblique projection methods for solving large unsymmetric systems*, SIAM Journal on Numerical Analysis, 19 (1982), pp. 485–506.

Reporter: Jörn Zimmerling

Participants

Prof. Dr. Harbir Antil

Department of Mathematical Sciences
George Mason University
4400 University Drive, MS: 3F2
Fairfax VA 22030-4444
UNITED STATES

Prof. Dr. Simon R. Arridge

Department of Computer Science
University College London
Gower Street
London WC1E 6BT
UNITED KINGDOM

Prof. Dr. Elena Beretta

Dipartimento di Matematica
Politecnico di Milano
Piazza Leonardo da Vinci, 32
20133 Milano
ITALY

Prof. Dr. George Biros

Oden Institute of Computational
Engineering and Sciences
The University of Texas at Austin
1 University Station C1200
Austin, TX 78712-1082
UNITED STATES

Prof. Dr. Liliana Borcea

Department of Mathematics
University of Michigan
530 Church Street
Ann Arbor, MI 48109-1043
UNITED STATES

Prof. Dr. Martin Burger

Department Mathematik
Universität Erlangen-Nürnberg
Cauerstrasse 11
91058 Erlangen
GERMANY

Prof. Dr. Fioralba Cakoni

Department of Mathematics
Rutgers University
Busch Campus, Hill Center
Piscataway, NJ 08854-8019
UNITED STATES

Dr. Maxence Cassier

Institut Fresnel, Université Aix-Marseille
Faculté des Sciences - Avenue Escadrille
13397 Marseille Cedex
FRANCE

Dr. Peng Chen

Oden Institute for Computational
Engineering and Sciences
The University of Texas at Austin
1 University Station C1200
Austin, TX 78712-1082
UNITED STATES

Prof. Dr. Christian Clason

Fakultät für Mathematik
Universität Duisburg-Essen
Mathematikcarrée
Thea-Leymann-Straße 9
45127 Essen
GERMANY

Prof. Dr. Maarten V. de Hoop

Simons Chair in Computational and
Applied Mathematics and Earth Science
Rice University
Houston TX 77005
UNITED STATES

Professor Vladimir L. Druskin

Worcester Polytechnic Institute
100 Institute Road
Worcester, MA 01609-2280
UNITED STATES

Prof. Dr. Herbert Egger
Fachbereich Mathematik
Technische Universität Darmstadt
Dolivostrasse 15
64293 Darmstadt
GERMANY

Prof. Dr. Josselin Garnier
Centre de Mathématiques Appliquées
École Polytechnique
91128 Palaiseau Cedex
FRANCE

Prof. Dr. Roland Griesmaier
Karlsruher Institut für Technologie
(KIT)
Institut für Angewandte und Numerische
Mathematik
Englerstrasse 2
76131 Karlsruhe
GERMANY

Dr. Fernando Guevara Vasquez
Department of Mathematics
University of Utah
155 South 1400 East
Salt Lake City, UT 84112-0090
UNITED STATES

Prof. Dr. Michael Hintermüller
Weierstraß-Institut für
Angewandte Analysis und Stochastik
Mohrenstrasse 39
10117 Berlin
GERMANY

Prof. Dr. Thorsten Hohage
Institut für Numerische und
Angewandte Mathematik
Universität Göttingen
Lotzestrasse 16-18
37083 Göttingen
GERMANY

Dr. Bangti Jin
Department of Computer Science
University College London
Gower Street
London WC1E 6BT
UNITED KINGDOM

Prof. Dr. Barbara Kaltenbacher
Institut für Mathematik
Alpen-Adria Universität Klagenfurt
Universitätsstrasse 65-67
9020 Klagenfurt
AUSTRIA

Dr. Tobias Kluth
FB 3 - Mathematik und Informatik
Zentrum für Technomathematik
Universität Bremen
Postfach 330 440
28334 Bremen
GERMANY

Prof. Dr. Peter Maaß
FB 3 - Mathematik und Informatik
Zentrum für Technomathematik
Universität Bremen
Postfach 330 440
28334 Bremen
GERMANY

Dr. Alexander Mamonov
Department of Mathematics
University of Houston
3551 Cullen Boulevard
Houston, TX 77204-3008
UNITED STATES

Prof. Dr. Anna Mazzucato
Department of Mathematics
Pennsylvania State University
305 McAllister Building
University Park, PA 16802
UNITED STATES

Prof. Dr. Shari Moskow
Department of Mathematics
Drexel University
Korman Center 269
3141 Chestnut Street
Philadelphia, PA 19104
UNITED STATES

Prof. Dr. Roman G. Novikov
CMAP UMR 7640 CNRS
École Polytechnique
91128 Palaiseau Cedex
FRANCE

Prof. Dr. Michael K. Pidcock
The School of Computing and
Mathematical Sciences
Oxford Brookes University
Wheatley Campus
Oxford OX33 1HX
UNITED KINGDOM

Hans-Georg Raumer
Deutsches Zentrum für Luft- und
Raumfahrt(DLR)
Institut für Aerodynamik und
Strömungstechnik
Bunsenstrasse 10
37073 Göttingen
GERMANY

Professor Kui Ren
Department of Applied Physics &
Applied Mathematics and Data Science
Institute
Columbia University
500 West 120th Street
New York, NY 10027
UNITED STATES

Prof. Dr. Arnd Rösch
Fakultät für Mathematik
Universität Duisburg-Essen
Thea-Leymann-Strasse 9
45127 Essen
GERMANY

Prof. Dr. Angkana Rüland
Mathematisches Institut
Universität Heidelberg
Im Neuenheimer Feld 205
69120 Heidelberg
GERMANY

Prof. Dr. William Rundell
Department of Mathematics
Texas A & M University
College Station, TX 77843-3368
UNITED STATES

Prof. Dr. Otmar Scherzer
Institut für Mathematik
Universität Wien
Oskar-Morgenstern-Platz 1
1090 Wien
AUSTRIA

Prof. Dr. Carola-Bibiane Schönlieb
Department of Applied Mathematics and
Theoretical Physics (DAMTP)
Centre for Mathematical Sciences
Wilberforce Road
Cambridge CB3 0WA
UNITED KINGDOM

Prof. Dr. John C. Schotland
Department of Mathematics
Yale University
Box 208 283
New Haven, CT 06520
UNITED STATES

Prof. Dr. Thomas Schuster
Fachrichtung Mathematik
Universität des Saarlandes
Postfach 151150
66041 Saarbrücken
GERMANY

Prof. Marian Slodicka

Department of Electronics and
Information Systems
Ghent University
Krijgslaan 281
9000 Gent
BELGIUM

Prof. Dr. Knut Solna

Department of Mathematics
University of California, Irvine
Irvine, CA 92697-3875
UNITED STATES

Prof. Dr. Georg Stadler

Courant Institute of Mathematical
Sciences
New York University
251, Mercer Street
New York, NY 10012-1110
UNITED STATES

Prof. Dr. Chrysoula Tsogka

Dept. of Applied Mathematics
University of California, Merced
5200 North Lake Road
Merced CA 95343
UNITED STATES

Prof. Dr. Daniel Wachsmuth

Mathematisches Institut
Universität Würzburg
Am Hubland
97074 Würzburg
GERMANY

JProf. Dr. Anne Wald

Institut für Numerische
und Angewandte Mathematik
Universität Göttingen
37083 Göttingen
GERMANY

Dr. Mikhail Zaslavsky

Schlumberger-Doll Research Center
1 Hampshire Street
Cambridge, MA 02139-1578
UNITED STATES

Dr. Zhidong Zhang

Sun Yat-sen University
Department of Mathematics
South Campus, Pu-Yuan District
Math. Building 607, Room 308 East 1.
Guangzhou 510275
CHINA

Dr. Jörn Zimmerling

Department of Mathematics
University of Michigan
530 Church Street
Ann Arbor, MI 48109-1043
UNITED STATES